frontiers in Environmental Chemistry

REVIEW
published: 22 September 2020
doi: 10.3389/fenvc.2020.00008

Recent Progress of Photocatalytic Fenton-Like Process for Environmental Remediation

Chencheng Dong, Mingyang Xing and Jinlong Zhang**

Key Laboratory for Advanced Materials and Joint International Research Laboratory of Precision Chemistry and Molecular Engineering, Feringa Nobel Prize Scientist Joint Research Center, Frontiers Science Center for Materiobiology and Dynamic Chemistry, School of Chemistry and Molecular Engineering, East China University of Science and Technology, Shanghai, China

Over the past few decades, Fenton process has been widely studied in environmental remediation. Due to the low efficiency of iron ions recycling, the Fenton efficiency has been seriously impeded for practical application. On this condition, with combination of photocatalysts, it is expected to fully use photo-generated electrons, thus enhancing the photo-Fenton efficiency. This synergistic methodology has assisted many researchers to remove various categories of organic pollutants in discharged wastewater or achieve gas conversion. This comprehensive review describes some significant advances with respect to presentative semiconductors (e.g., TiO_2, g-C_3N_4, graphene, $BiVO_4$, $ZnFeO_4$ and $BiFeO_3$, etc.) including their preparation methods, characterization and applications in environmental remediation (e.g., organic removal, bacteria disinfection, membrane separation, and gas conversion). The mechanism is preferentially discussed. Possibly future development and its correlated potential challenges are specifically proposed and discussed in this review.

Keywords: photocatalytic Fenton reaction, organic pollutant degradation, disinfection, volatile organic compound (VOC), membrance

OPEN ACCESS

Edited by:
Qizhao Wang,
Northwest Normal University, China

Reviewed by:
Yanhui Ao,
Hohai University, China
Xufang Qian,
Shanghai Jiao Tong University, China
Mingshan Zhu,
Jinan University, China

****Correspondence:***
Mingyang Xing
mingyangxing@ecust.edu.cn
Jinlong Zhang
jlzhang@ecust.edu.cn

Specialty section:
This article was submitted to Catalytic Remediation, a section of the journal Frontiers in Environmental Chemistry

Received: *08 July 2020*
Accepted: *11 August 2020*
Published: *22 September 2020*

Citation:
Dong C, Xing M and Zhang J (2020) Recent Progress of Photocatalytic Fenton-Like Process for Environmental Remediation. Front. Environ. Chem. 1:8. doi: 10.3389/fenvc.2020.00008

INTRODUCTION

In recent decades, the aqueous environment arising from a great variety of contaminants, for instance, emerging contaminants (ECs) including pharmaceuticals and personal care products (PPCPs), dyes, endocrine-disrupting compounds (EDCs), flame retardants (FRs), pesticides, and their metabolites pose a major concern to human beings (Esplugas et al., 2007; Klamerth et al., 2013). Although their concentration in real sewage is in the $\mu g\ L^{-1}$-$ng\ L^{-1}$ range, they unconsciously discharge into the environment and biologically accumulate in human body, thus posing a severe threat to receiving waters (e.g., rivers, aquifers and groundwater) (Zhang et al., 2014). To the best of our knowledge, conventional wastewater treatment plants (WWTP) are often unable to entirely degrade persistent organic pollutants (Jelic et al., 2011; Klamerth et al., 2013). Consequently, the pollutants and their metabolites accumulate in the aquatic environment, indirectly they may cause ecological risk. As a result, the alternatively advanced technique is of paramount importance to be developed.

Advanced oxidation processes (AOPs), which have been proposed as replaceable solutions for degrading persistent organic compounds, because the hydroxyl radicals (·OH) are

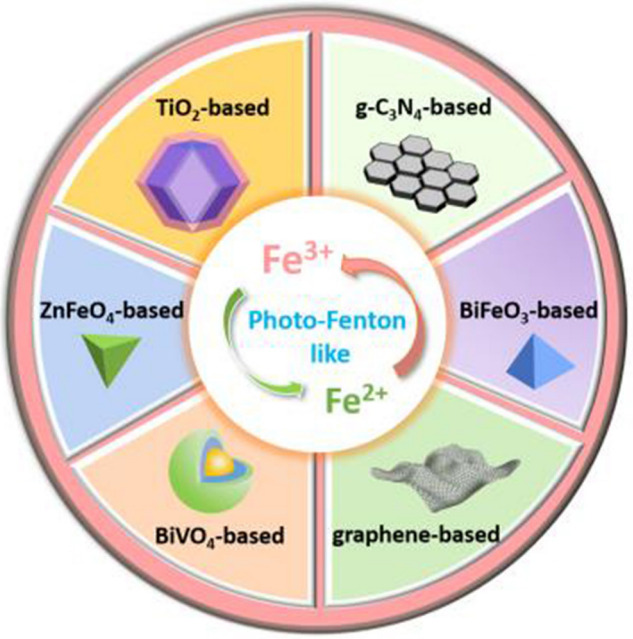

Graphical Abstract | Semiconductor-based photo-Fenton like nanomaterials.

unselectively promote organic substances oxidation at high reaction rates (Zhang et al., 2009; Sun et al., 2020). Besides this, AOPs are also called as versatile technologies owing to the various alternative ways in generation hydroxyl radicals (Lee and von Gunten, 2010). In comparison with conventional treatment techniques, AOPs are more efficient and capable of degrading recalcitrant pollutants. In AOPs, a variety of oxidants such as hydrogen peroxide (H_2O_2) (Dong C. et al., 2018; Xing et al., 2018a), persulfate (Matzek and Carter, 2016; Wang and Wang, 2018), peroxymonosulfate (Shao et al., 2017; Tan et al., 2017; Duan et al., 2018; Lei et al., 2019; Ma et al., 2019; Shen et al., 2019), permanganate (Guo et al., 2018; Chow and Sze-Yin Leung, 2019; Wang et al., 2019), and ozone (O_3) (Khan et al., 2017; Ikehata and Li, 2018) have been employed to degrade organic matters. Among these oxidants, H_2O_2 has been widely recognized as economically and environmentally friendly oxidant, according to its high efficacy and environmental friendliness.

In short, the combination of Fe^{2+} and H_2O_2 are called conventional Fenton reaction, which belong to a type of classical AOPs. Since 1894, H.J.H Fenton proposed the concept of Fenton process, he found that Fe^{2+} and H_2O_2 could degrade tartaric acid. Thus, it has been widely used in environmental remediation in the following decades (Jain et al., 2018). As the merits of Fenton progress, it is normally operated under ambient temperature and pressure (Qian et al., 2017, 2018a), and generate strongly oxidizing radical species (primarily ·OH) for the complete decomposition of organic pollutants into non-toxic products, such as CO_2, H_2O and inorganic salts (Dong C. et al., 2018). Besides this, the advantages of Fenton process over other WWTPs are extremely superior, including of higher removal efficiency, no residues and wide region for treating substances as well as no need of special equipment. The conventional Fenton mechanism, which is involved with Fe^{2+}/H_2O_2, is exhibited as the following equations:

$$Fe^{2+} + H_2O_2 \rightarrow Fe^{3+} + OH^- + \cdot OH \quad k_1 = 40\sim80 L\cdot mol^{-1}\cdot S^{-1} \quad (1)$$

$$Fe^{3+} + H_2O_2 \rightarrow Fe^{2+} + \cdot O_2H^- + H^+ \quad k_2 = 9.1^{*}10^{-7} L\cdot mol^{-1}\cdot S^{-1} \quad (2)$$

$$Fe^{3+} + \cdot O_2H^- \rightarrow Fe^{2+} + O_2 + H^+ \quad k_3 = 0.33\sim2.1^{*}10^{6} L\cdot mol^{-1}\cdot S^{-1} \quad (3)$$

However, the conventional decomposition efficiency of H_2O_2 in Fe^{2+}/H_2O_2 system is constrained by the low Fe^{3+}/Fe^{2+} cycle, owing to the low reaction rate constant of Equation (2). Therefore, the key to enhance the Fenton efficiency is accelerating the reaction constant of Equation (2); meanwhile, the iron sludge will be greatly reduced due to the high efficacy of Fe^{3+}/Fe^{2+} cycle.

Besides Fenton process, photocatalytic oxidation has been considered as alternative and efficient AOP as well. Photocatalysis based AOPs initiate the complex chain reactions, and it may produce the colorless organic intermediates. Correspondingly, these colorless intermediates maybe more toxic than the parent molecular. Additionally, all of the Fenton reactions including conventional Fenton process and Fenton-like or photo-Fenton-like process easily produce iron mud, and it needs a large amount of manpower and chemicals to treat and remove iron mud. Thus, to achieve a thorough mineralization of organic compound is the main goal of AOPs in environmental remediation. After retrospection of the past few decades, it can be found that many studies have utilized the nano-photocatalysts for the degradation of organic pollutants; however, the utilization efficiency of photo-generated electrons and holes still remains a challenge for researchers in WWTPS. Based on this background information, many researchers have coupled Fenton reaction with photocatalysis as a novel technique to treat wastewater, which can be assigned to novel Fenton-like reaction. By means of this, it is able to realize a win-win situation. To be more specific, it can not only prolong the lifetime of photo-generated carries [i.e., photo electrons (e^-) and hole (h^+)], but also the photo-generated electrons will accelerate the cycle of Fe^{3+}/Fe^{2+}, leading to higher mineralization of pollutant and the reduction of iron sludge.

In this paper, we mainly review and summary several representative nanomaterials, which have been applied in photocatalytic Fenton reaction, including of TiO_2-based, g-C_3N_4-based, reduced graphene oxide (RGO)-based and other semiconductors-based nanomaterials (e.g., Ag, $BiVO_4$, $ZnFeO_4$, and $BiFeO_3$ based nanomaterials). This review mainly aims to review the nanomaterials based AOPs that are used for degradation of different organic pollutants in wastewater or volatile organic compounds (VOCs) removal and provide some effective information for developing latest solution of WWTPs.

TiO_2-BASED PHOTOCATALYTIC FENTON REACTION

Removing Organic Pollutant

Since 1972, Fujishima and Honda (1972) found that titanium oxide (TiO_2) could split water to produce hydrogen under UV light irradiation, thus opening up a new era of titanium oxide (TiO_2) in photocatalysis. Up to now, TiO_2 has been

TABLE 1 | Summary of TiO_2 based heterogeneous photo-Fenton and photo-Fenton like process under light irradiation.

Catalyst	Target pollutant	pH	Catalyst dose	H_2O_2 dose	Reaction time	Light source	Decolorization	References
$ZnSe/TiO_2$	10 mg/L pentachlorophenol	5.0	100 μM Fe^{3+}	75 μM	120 min	Solar light	99% discoloration	ThanhThuy et al., 2013
Fe-VT	100 mg/L orange X-GN	3.0	0.5 g/L	3.92 mM	80 min	UV light	98.7% discoloration,54.4% TOC removal	Chen et al., 2010
TiO_2	40 ppm 3-chloropyridine	2.8	0.88 mM Fe^{2+}, 700 mg/L TiO_2	8.8 mM	60 min	UV light	100% TOC removal	Ortega-Liébana et al., 2012
TiO_2	0.1 mM phenol and benzoic acid	6.0	0.25 mM Fe (III), 1.0 g/L TiO_2	10 mM	120 min	UV light	phenol 100%, BA: 96%	Kim et al., 2012
$Fe\text{-}TiO_2$	2.1×10^{-4} mol L^{-1} phenol	6.4	0.2 g/L	0.015 mM	300 min	UV light	20%	Tryba et al., 2006
$Fe\text{-}C\text{-}TiO_2$	2.1×10^{-4} mol L^{-1}phenol	2.8	0.2 g/L	0.015 mM	120 min	UV light	98% degradation removal	Tryba et al., 2006
$Fe\text{-}TiO_2$	0.32 mM thiacloprid	2.8	1.67 g/L	45 mM	500 min	UV light	100% TOC removal	Banić et al., 2011
$CdS/MWCNT\text{-}TiO_2$	50 mM methylene blue	3.5	0.75 g/L	0.6 mM	120 min	Visible light	98% discoloration and 83% TOC removal	Kim and Kan, 2015

well-applied in the fields of energy and environment, including organic removal (Vaiano et al., 2015; Shayegan et al., 2018; Chen et al., 2019; Dong et al., 2019), hydrogen production (Zhang et al., 2012; Xi et al., 2014; Xing et al., 2015; Zhou Y. et al., 2016), CO_2 reduction (Yu et al., 2014; Dong et al., 2018a; Xing et al., 2018b), nitrogen fixation (Comer and Medford, 2018; Li C. et al., 2018; Zhao et al., 2019), and methane conversion (Wang P. et al., 2017; Yu et al., 2017), etc. Attributed to the sufficiently high reduction potential, low economical cost and high stability, TiO_2 has attracted great attention as one of the most potential and influential photocatalysts (Dong et al., 2018b). In terms of photocatalytic Fenton reaction, especially, TiO_2 based nanomaterials have been developed. Consequently, Photo-Fenton oxidation process employed modified TiO_2, Fe^{2+}or Fe^{3+}, and H_2O_2 under light irradiation, leading to significant improved generation of hydroxyl radicals and degradation efficiency of organic pollutants owing to synergy between photocatalysis and Fenton reaction. Some examples have been summarized in **Table 1**.

In **Table 1**, we have listed some representative work in recent years. In 2012, Ortega-Liébana et al. (2012) developed $Fe^{2+}/TiO_2/H_2O_2$/UV system for the degradation of 40 ppm 3-chloropyridine. The results showed that photo-Fenton process is more efficient than sole TiO_2 photocatalysis, which meant that this technique possessed more practical industrialized application than photocatalysis. As to some modified TiO_2 nanomaterials, for instance, Tryba et al. (2006) prepared $Fe\text{-}TiO_2$ and $Fe\text{-}C\text{-}TiO_2$ nanomaterials, which could effectively degrade phenol. The highly efficient decomposition of phenol on $Fe\text{-}C\text{-}TiO_2$ photocatalysts mainly attributed from several factors: (1) the produced hydroxyl radicals in Fenton process; (2) the reduction of Fe^{3+} back to Fe^{2+} under UV light; (3) the cocatalytic effect of hydroquinone. Additionally, Banić et al. (2011) prepared Fe/TiO_2 materials with various loading amount of Fe_2O_3 nanoparticles. The $7.2Fe/TiO_2/H_2O_2$ system exhibited the highest activity for removing TCL among all the used AOPs (**Figures 1A,B**). In **Figure 1A**, it could be observed that 1.67 g L^{-1} $7.2Fe/TiO_2$/45 H_2O_2 system achieved 100% removal efficiency after 25 min. However, in this case, TiO_2 only acted as a good support, because the degradation efficiency of $7.2Fe/TiO_2$ is lower compared to the TiO_2 support, indicating the presence of Fe under UV irradiation did not contribute to the catalytic activity of the material, and not facilitating the cycle of Fe^{3+}/Fe^{2+}. Moreover, the results indicated that the removal efficiency was influenced by some possible parameters including pH and TCL concentrations (**Figures 1C,D**). In **Figure 1C**, the optimal pH value was fixed at 2.8. As to TCL concentrations, when TCL concentration exceeded 0.12 mM, the reaction rate tended to slow down (**Figure 1D**), ascribed to that most of the $7.2Fe/TiO_2$ active sites were occupied, leading to reduced generation of reactive oxygen species.

When it comes to coupled semiconductor, ThanhThuy et al. (2013) prepared $ZnSe/TiO_2$ nanocomposites. Under simulated solar light, the ZnSe sensitized TiO_2 nanotube arrays exhibited remarkable capability for photocatalytic degradation of pentachlorophenol assisted with photo-Fenton system (i.e., Fe^{3+}/H_2O_2/humic acid). The results showed that 99.0% of pentachlorophenol could be degraded in comparison with pure TiO_2 NTAs (64.0%) after 2 h solar light irradiation. Further, Kim and Kan (2015) synthesized CdS/carbon nanotube-TiO_2 ($CdS/CNT\text{-}TiO_2$), which was applied in heterogeneous photo-Fenton process as well. The heterogeneous photo-Fenton oxidation cocatalyzed by $CdS/CNT\text{-}TiO_2$ was mainly engaged in the combination of the photocatalytic, photo-Fenton and photosensitizing oxidation. Consequently, the photo-Fenton process achieved a high decolorization (98%) and mineralization rate (83%). To the best of our knowledge, the concentration of ferrous and ferro ferric ion as well as hydrogen peroxide is of great necessary for enhancing treatment efficiency and minimizing operating costs. In **Figure 2A**, firstly, it was found

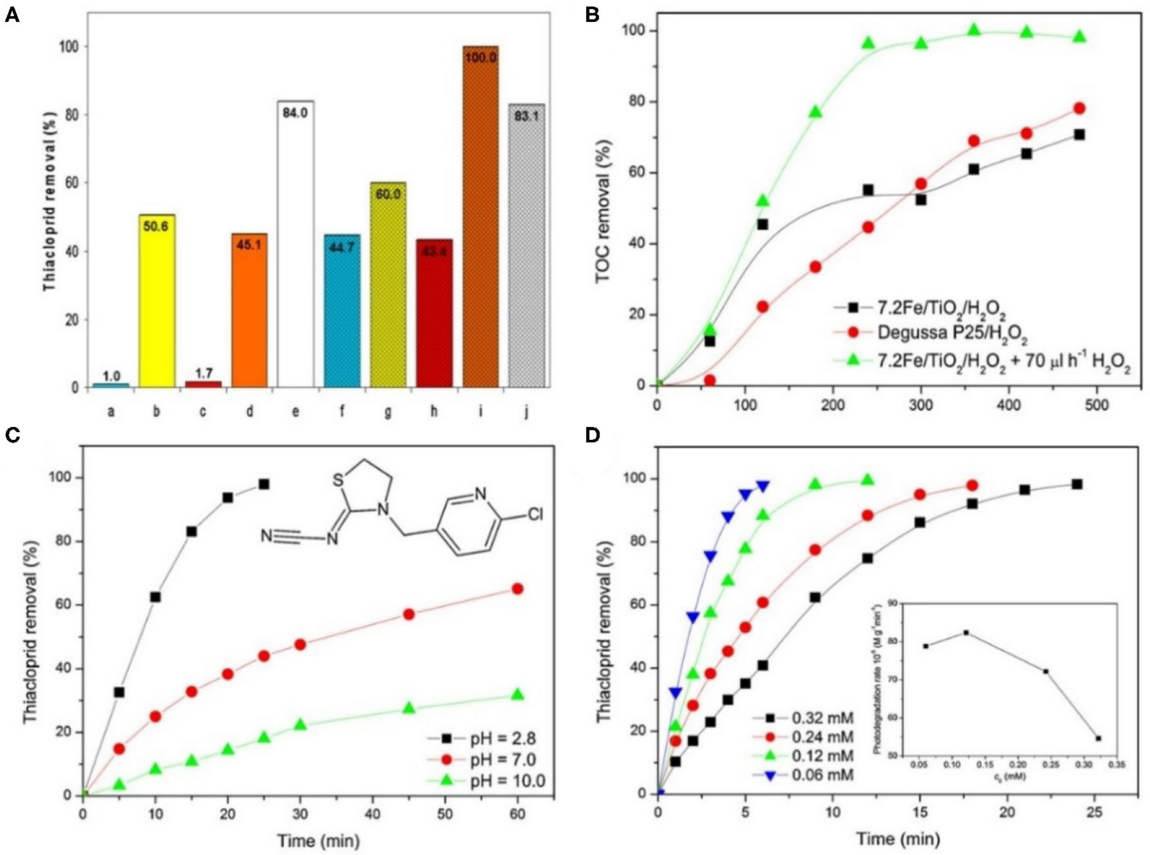

FIGURE 1 | (A) Photodegradation efficiency of various systems of TCL under UV light irradiation: (a) photolysis, (b) TiO_2 support, (c) PrecFe, (d) 7.2Fe/TiO_2, (e) Degussa P25, (f) H_2O_2, (g) TiO_2 support/H_2O_2, (h) PrecFe/H_2O_2, (i) 7.2Fe/TiO_2/H_2O_2, and (j) Degussa P25/45 mM H_2O_2. **(B)** TOC removal efficiency for TCL in the presence of 7.2Fe/TiO_2 and Degussa P25, respectively. **(C)** Impact of pH value on the kinetic of TCL photodegradation efficiency. **(D)** Impact of TCL concentration on the kinetic photodegradation efficiency (inset picture: the impact of the TCL concentration on the TCL degradation rate at 6 min light irradiation). Copied with permission (Banić et al., 2011). Copyright 2011, Elsevier.

that degradation and TOC removal efficiency of MB can be increased to 99 and 83%, respectively. Secondly, the ratio of $[Fe^{3+}]$: $[H_2O_2]$ increased from 0.05 to 0.5 led to the MB removal efficiency to 100%; meanwhile, the TOC removal efficiency could be increased from 61 to 84% (**Figure 2B**). The detailed mechanism has been proposed in **Figure 2C**. Specifically, the photo-induced electron (e^-_{cb}) on the surface of TiO_2 can be scavenged by oxygen, whereas the photo-induced hole (h^+_{vb}) can react with OH^- or H_2O. Afterwards, the electrons transferred to these adsorb Fe^{3+} ions on TiO_2 surface, leading to the cycle of Fe^{3+}/Fe^{2+}. Simultaneously, the electron on TiO_2 surface would possibly impede the electron-hole recombination. Lastly, MB molecular acting as photosensitizer would form MB* under visible light irradiation. The electron transfer between the MB* and Fe^{3+} would be beneficial to regenerating Fe^{2+}, which accelerated the kinetic rate of the photo-Fenton process.

Disinfection

Apart from the organic pollutant removal, photo-Fenton process serving for water disinfection has emerged in recent decades. Commonly, according to the rules, two main solutions are able to be adopted if researchers want to employ photo-Fenton process to bacterial inactivation, including of drinking water disinfection and secondary effluent from municipal wastewater treatment plants (MWWTPs) (Giannakis et al., 2016). In terms of the target microorganisms, especially *E. coli* K12, was mostly selected as studied target. Regarding TiO_2 on disinfection, the earliest systematic study was reported mainly based on photocatalytic water disinfection for *E. coli* inactivation (Rincón and Pulgarin, 2004a,b). Afterwards, Rincón and Pulgarin (2006) compared Fe^{3+} and TiO_2 assisted system. Several systems have been established (e.g., UV-vis/TiO_2, UV-vis/TiO_2/H_2O_2, UV-vis/Fe^{3+}/H_2O_2, and UV-vis/H_2O_2). It was revealed that the disinfection rate of TiO_2 could be accelerated if H_2O_2 existed. Herein, TiO_2 itself can show disinfection efficiency of *E. coli*, acting as photocatalyst, which can produce hydroxyl radicals under UV-vis irradiation. After addition of H_2O_2, the photoinduced charge transfer will be effectively separated because H_2O_2 acting as electron acceptor, thus preventing the recombination of electron-hole pairs, and generating much

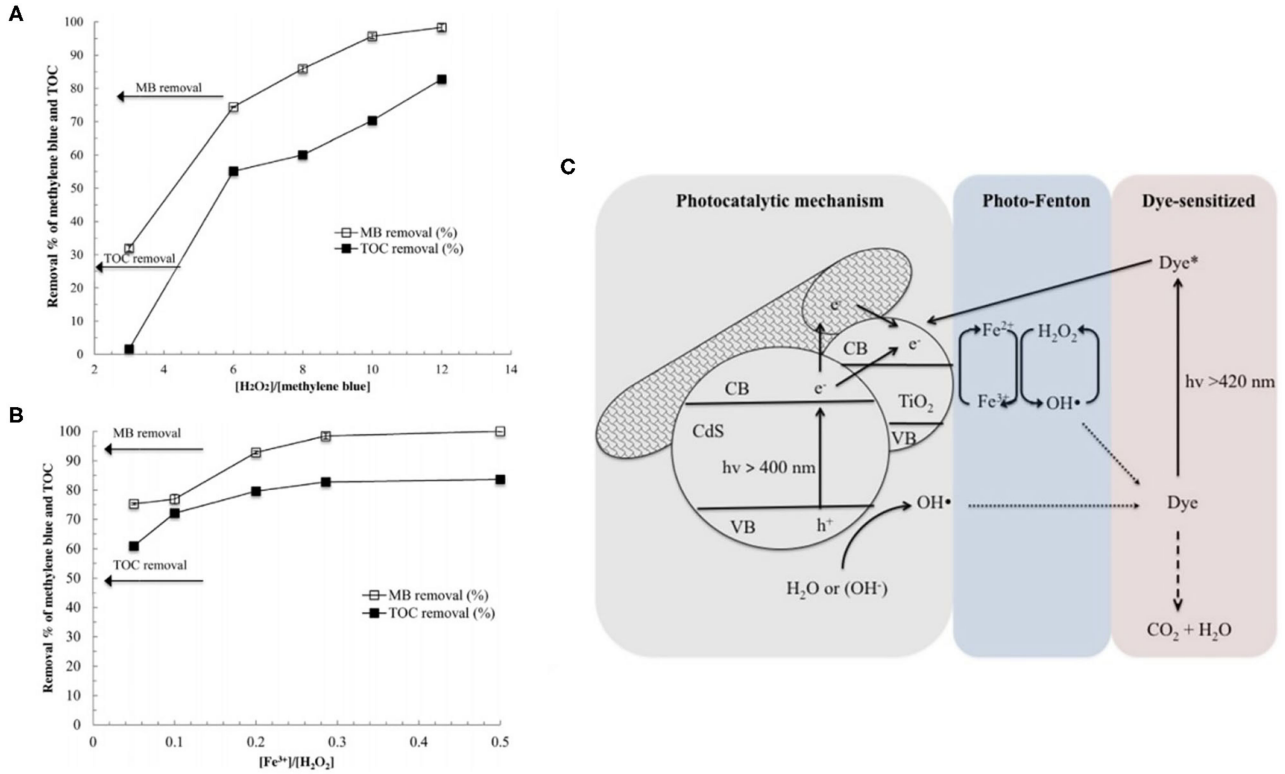

FIGURE 2 | (A) Impact of the ratio of $[H_2O_2]$/[MB] on photo-Fenton degradation efficiency of MB. **(B)** Impact of the ratio of $[Fe^{3+}]/[H_2O_2]$ on photo-Fenton degradation efficiency of MB. **(C)** Proposed mechanism of CdS/CNT-TiO_2 for photo-Fenton degradation of MB under visible light irradiation. Copied with permission (Kim and Kan, 2015). Copyright 2015, Elsevier.

more ·OH radicals. In **Figure 3A**, it could be clearly seen that TiO_2/H_2O_2 system is more efficient than Fe^{3+}/H_2O_2 system. Compared to the dark controls in **Figure 3B**, the irradiation of solar light could promote the bacterial inactivation. H_2O_2 alone did not obviously impede the *E. coli* survival, whereas TiO_2 could increase its bactericide oxidation ability.

In this section, TiO_2 based nanomaterials have been briefly introduced in the field of organic pollutant removal and disinfection of bacteria in wastewater. Regarding of this, TiO_2 based nanomaterial is expected to perform as well as in actual usage.

g-C_3N_4-BASED PHOTOCATALYTIC FENTON REACTION

Due to the simple synthesis method, good physical and chemical stability and earth abundant characteristics, graphite carbonitride (g-C_3N_4) has attracted scientists attention in terms of energy conversion and environmental remediation (Lan et al., 2019). As to homogeneous Fe^{2+}/H_2O_2 Fenton process, the water-soluble Fe^{2+} catalyzed H_2O_2 to produce hydroxyl radical; however, traditional homogeneous catalysts will be constrained by the following drawbacks: (1) low decomposition efficiency of H_2O_2; (2) sludge residue; (3) limited pH value between 3.0 and 4.0 (Qian et al., 2018b). Overall, iron leaching issue has posed serious problem in acidic aquatic environment. Additionally, g-C_3N_4 nanomaterials have emerged as a promising visible-light-response photocatalyst in organic removal and water splitting (Dong H. et al., 2018; Safaei-Ghomi et al., 2019). In 2012, Cui et al. (2012) firstly reported that visible light excited of g-C_3N_4 catalyzed H_2O_2 to produce ·OH radicals. Successively, g-C_3N_4 coupled with various types of Fe-based materials were explored for removing recalcitrant organic pollutants via photo-Fenton process, including of iron minerals (He et al., 2017), Fe(III) (Hu et al., 2016), single molecule iron complex (Chen et al., 2010; Banić et al., 2011), and iron oxide (Zhou L. et al., 2016; Wang et al., 2018) etc. Moreover, carbon nitride-based nanomaterials could serve as photo-Fenton-like membranes (Yu et al., 2018; Lan et al., 2019). Except of above mentioned, Li et al. (2016) constructed solid-gas-interfacial Fenton reaction over alkalinized-C_3N_4 photocatalyst in isopropanol photodegradation. The specific illustration will be revealed in this section.

Removing Organic Pollutant

Regarding photo-Fenton degradation of refractory organic pollutants, notably, Zhou L. et al. (2016) has built a highly efficient visible-light-driven heterogeneous photo-Fenton system (i.e., Fe_2O_3/g-C_3N_4/H_2O_2), which demonstrated that Fe_2O_3 nanoparticles were uniformly dispersed onto the surface of g-C_3N_4 (**Figure 4A**) and formed a heterojunction with g-C_3N_4

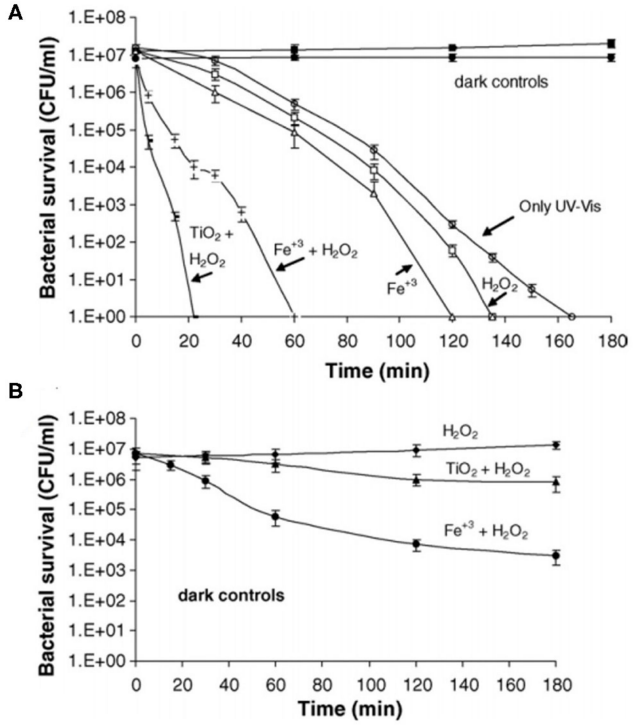

FIGURE 3 | (A) *E. coli* inactivation under different light driven AOPs systems including UV-vis/TiO_2/H_2O_2, UV-vis/Fe^{3+}/H_2O_2, UV-vis/Fe^{3+}, UV-vis/H_2O_2, and only UV-vis. Dark controls: Fe^{3+} and TiO_2. **(B)** *E. coli* survival under different dark systems including of TiO_2/H_2O_2, Fe^{3+}/H_2O_2, and H_2O_2 systems. Copied with permission (Rincón and Pulgarin, 2006). Copyright 2006, Elsevier.

to enhance the charge separation. It can be clearly observed that Fe_2O_3 nanoparticles uniformly dispersed onto g-C_3N_4 nanosheets in comparison with pristine g-C_3N_4 (**Figure 4B**). As to degradation efficiency, the result was clarified in **Figure 4C**. The photo-Fenton capacity of Fe_2O_3/g-C_3N_4 was investigated for removing MO aided by H_2O_2 under visible-light irradiation. From the figure curves, it can be obtained that all the Fe_2O_3/g-C_3N_4 exhibited superior degradation efficiency than pure Fe_2O_3 and g-C_3N_4 as well as g-C_3N_4+Fe_2O_3. The absorbance intensity of MO decreased gradually with time as shown in **Figure 4D**. Moreover, the kinetic constant of photo-Fenton degradation efficiency of Fe_2O_3/g-C_3N_4 was determined as shown in **Figure 4E**. Significantly, the *k*-value of Fe_2O_3/g-C_3N_4 is about 45.4 times higher than that of Fe_2O_3, 8.4 times higher than that of g-C_3N_4 and 7.2 times than that of g-C_3N_4+Fe_2O_3, respectively. Based on experimental analysis, a possible mechanism is proposed in **Figure 4F**. Once irradiated with visible light, the electron-hole pairs will be produced from both of Fe_2O_3 and g-C_3N_4; meanwhile, the interfacial charge transfer promoted by the contact between Fe_2O_3 and g-C_3N_4 will further enhance the charge separation efficiency. The highly efficient efficiency not only arose from the photo-generated holes reacting with water molecular to produce hydroxyl radicals, but also the photo-induced electrons will be utilized to produce hydroxyl radicals. The generated electrons in the CB of Fe_2O_3 and transferred from the CB of g-C_3N_4 will contributed the conversion between Fe^{3+} and Fe^{2+}. Overall, the generation rate of hydroxyl radicals which produced during Fenton process will be accelerated, thus leading to the enhancement of degradation efficiency. In addition, the fully consumption of photo-induced electrons during Fenton process will ulterior promote the charge separation, introducing more holes devoting to degradation process. Lastly, the catalytic activity can be greatly enhanced if photocatalysis technique joint with Fenton process were employed in one system.

Differentiate with the sole Fe_2O_3 nanoparticles, Guo et al. (2019) constructed a Z-scheme hetero-structured α-Fe_2O_3@g-C_3N_4 catalyst, which was obtained by calcination of melamine and Fe-based MOF. Commonly, MOFs are mainly used to prepare metal oxide nanoparticles, which can inherit the merits of metal oxide acting as sacrifice templates. The morphology characterization has been shown in **Figure 5A**. Regarding the TC degradation efficiency, by adjusting the addition amount of MIL-53 (Fe), the researchers obtained the optimized composite, which exhibited excellent photo-Fenton performance for the removal of TC (**Figure 5B**). The corresponding degradation kinetic rate was calculated in **Figure 5C**, the *k*-value of FOCN-0.45 (0.042 min^{-1}) was 6, 7, and 14 times, compared to that of pristine MIL-53 (Fe) ($k = 0.007\ min^{-1}$), α-Fe_2O_3 ($k = 0.006\ min^{-1}$), and g-C_3N_4 ($k = 0.003\ min^{-1}$), respectively. As to reactive species, the scavenger results in **Figure 5D** demonstrated that ·OH was the dominant species, accompanied with $O_2^{\cdot-}$ and h^+ co-participating in the degradation of TC. The specific mechanism of photo-Fenton reaction over Z-scheme hetero-structured α-Fe_2O_3@g-C_3N_4 was shown in **Figure 5E**. Generally, g-C_3N_4 and α-Fe_2O_3 can be both excited under visible light (420 nm) irradiation to produce photo-induced electron (e–) and hole (h+). Owing to the Z-scheme structure, a proportion of electrons of the CB of α-Fe_2O_3 would be prone to transferring to the VB of g-C_3N_4. The electron of CB for g-C_3N_4 would react with O_2 to produce superoxide radicals to degrade pollutants. Because of the CB position of α-Fe_2O_3 more negative than the standard potential of Fe^{3+}/Fe^{2+} (0.77 V vs. NHE), thus the electrons of α-Fe_2O_3 were able to participate in the cycling of Fe^{3+}/Fe^{2+}, leading to activating H_2O_2 to generate hydroxyl radical. As to the holes in the VB of α-Fe_2O_3, the VB position of α-Fe_2O_3 (1.98 V vs. NHE) was lower than the potential of $OH^-/\cdot OH$ (1.99 V vs. NHE). Consequently, the accumulated holes in the VB of α-Fe_2O_3 directly degraded the organic pollutants.

Furthermore, some other novel g-C_3N_4 based nanomaterials have been progressed in photo-Fenton application. For instance, Palanivel et al. (2019) rationally designed an effective heterostructure ($ZnFe_2O_4$/g-C_3N_4) nanocomposite, which showed good photo-Fenton performance for degradation of 20 mg/L MB. Besides Fe_2O_3 nanoparticles, Sahar et al. (2017) prepared Fe_3O_4/g-C_3N_4 nanoparticles mainly throughout electrostatic self-assembly effect, exhibiting an obviously enhanced Fenton, photo-Fenton and peroxidase-like efficiency. To achieve the goal of easy access of recycling, Wang H. et al. (2017) synthesized magnetic $BaFe_{12}O_{19}$/g-C_3N_4 nanocomposites, which showed excellent capacity and recyclability for removing RhB. The enhanced photocatalytic performance was mainly attributed to the synergy of $BaFe_{12}O_{19}$

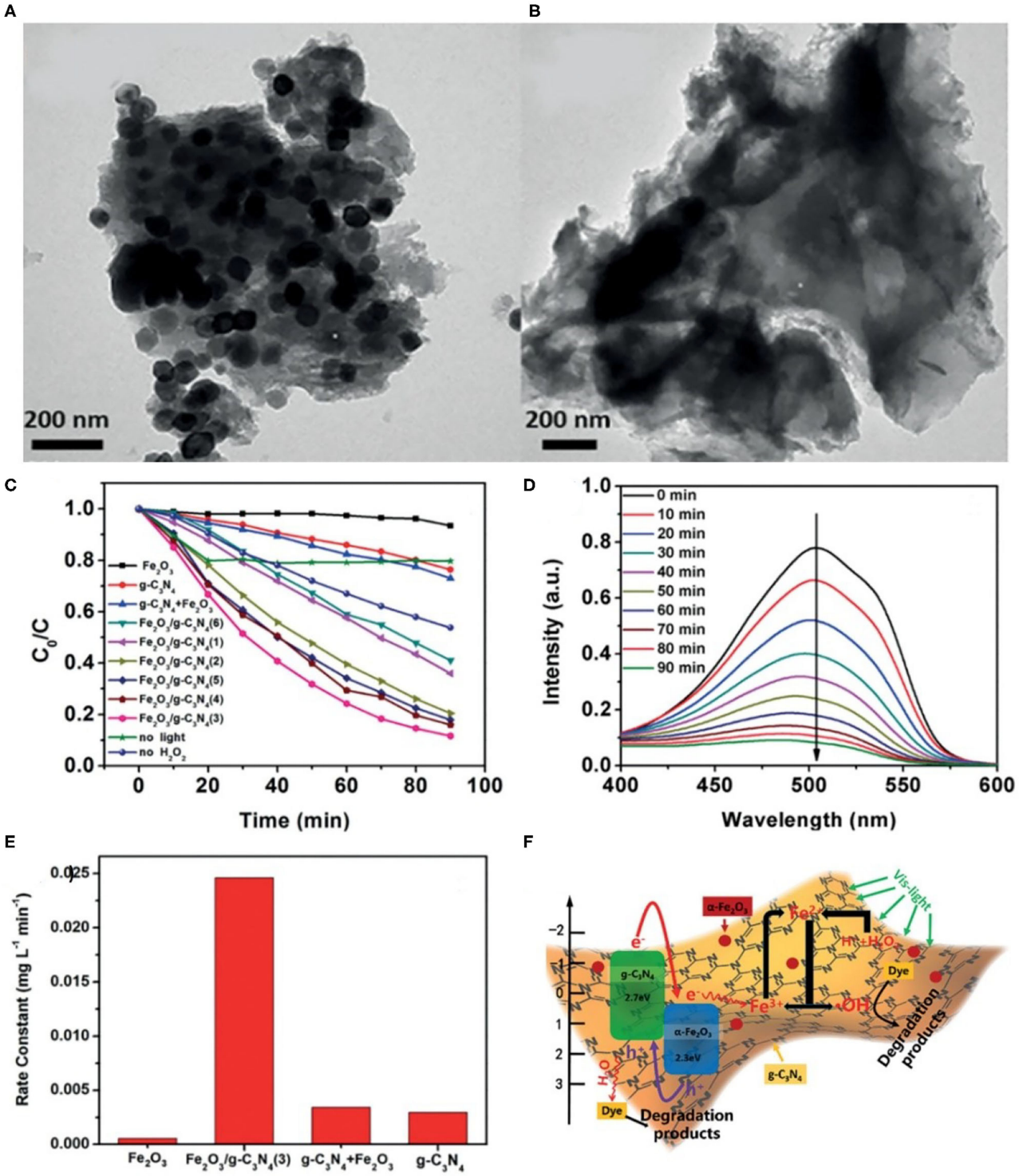

FIGURE 4 | (A) TEM images of $Fe_2O_3/g\text{-}C_3N_4$ and **(B)** $g\text{-}C_3N_4$. **(C)** Photo-Fenton degradation efficiency of various catalysts for 20 mg L^{-1} MO under visible light irradiation. **(D)** UV/Vis spectra of MO of $Fe_2O_3/g\text{-}C_3N_4$ at different time intervals. **(E)** Corresponding rate constant of various catalysts. **(F)** Proposed mechanism in the photo-Fenton reaction. Copied with permission (Zhou L. et al., 2016). Copyright 2016, Wiley.

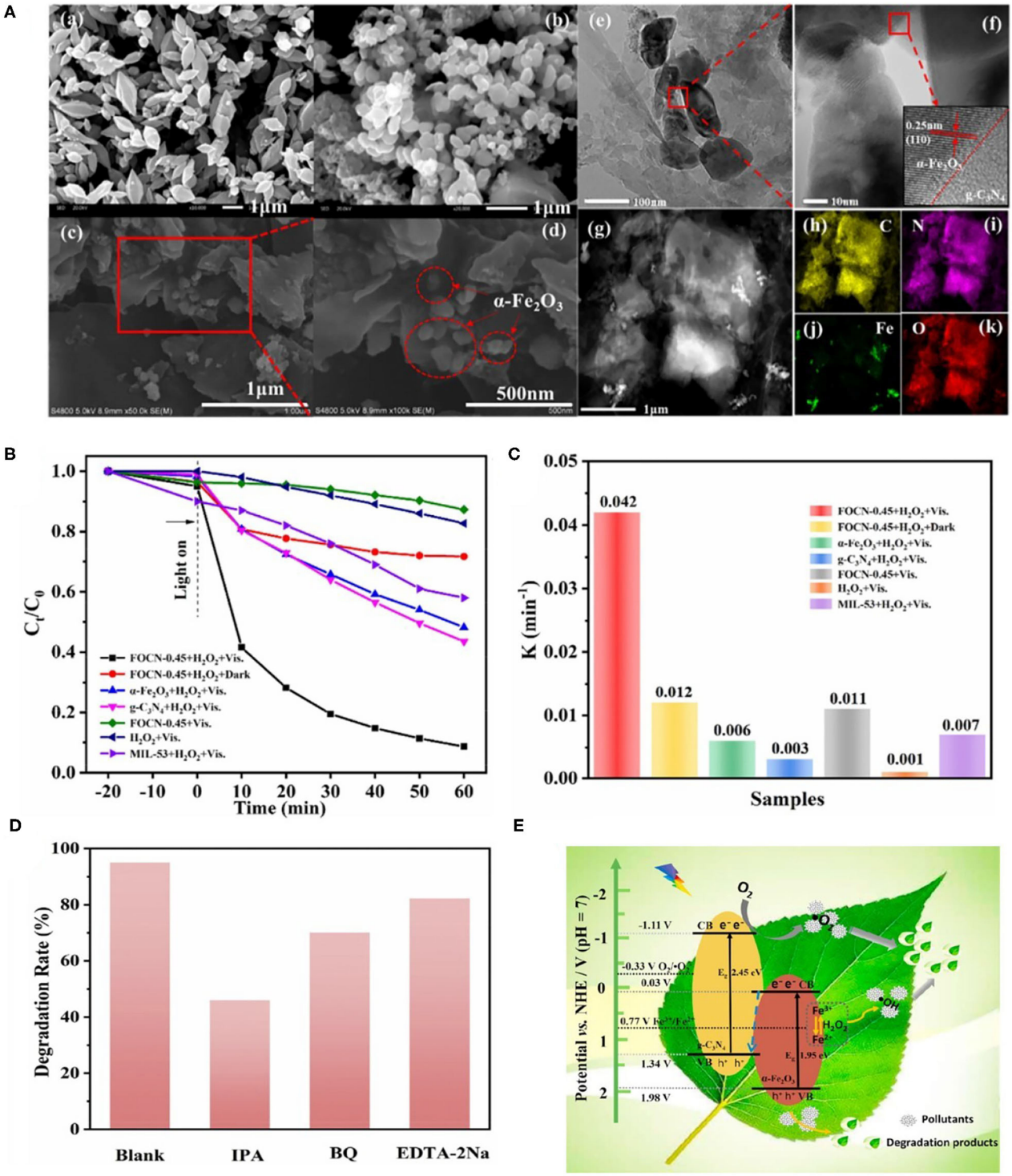

FIGURE 5 | (A) SEM images of MIL-53 (Fe) (a), α-Fe_2O_3 (b), (c) FESEM image of FOCN-0.45 and its amplified area (d); (e) TEM and HRTEM (f) images of FOCN-0.45, (g) HAADF-STEM image; (h–k) corresponding EDX mapping of FOCN-0.45. **(B)** TC degradation efficiency of different samples. **(C)** Kinetic calculation of various samples at different conditions. **(D)** Scavenger test of FOCN-0.45 for removing TC. **(E)** Photo-Fenton reaction mechanism illustration of α-Fe_2O_3@ g-C_3N_4 heterojunction. Copied with permission (Palanivel et al., 2019). Copyright 2019, Elsevier.

TABLE 2 | Summary of C_3N_4 based heterogeneous photo-Fenton like process under visible light irradiation.

Catalyst	Target pollutant	pH	Catalyst dose	H_2O_2 dose	Reaction time	Decolorization	References
g-C_3N_4/FeOCl	50 mg/L tetracycline 10 mg/L rhodamine B	/	0.2 g/L 0.2 g/L	2 mM	60 min	90%	Zhao et al., 2020
g-C_3N_4-IMD-$FePcCl_{16}$	Carbamazepine (CBZ)	7.0	0.1g/L	5 mM	100 min	100%	Chen X. et al., 2017
g-C_3N_4/$LaFeO_3$	10 mg/L rhodamine B	/	0.5 g/L	5 mM	120 min	100%	Ye et al., 2018
Fe-doped g-C_3N_4	20 mg/L phenol, bisphenol A, 2, 4dichlorophenol	/	1.0 g/L	8.0 mM	50 min	100%	Hu et al., 2019
Oxygen doping C_3N_4 (HS g-C_3N_4-O)	Rhodamine B	/	0.5 mg cat, 1.0 mM $FeCl_3$	20 mM	50 min	100%	Guo et al., 2016
$Cu_2(OH)PO_4$/g-C_3N_4	10 mg L^{-1} RhB	/	0.02 g cat	10 mM	40 min	100%	Chen et al., 2015
$Zn_{1-1.5x}Fe_xS$/g-C_3N_4	10 mg/L p-nitrophenol (PNP)	/	0.8 g/L	1 mM	60 min	96%	Wang et al., 2020
Fe-g-C_3N_4/GMC	50 mg/L Acid Red 73	/	0.8 g/L	40 mM	40 min	99.2%	Ma et al., 2017

and g-C_3N_4, thus facilitating charge separation, and thereby promoted the photo-Fenton efficiency. For more examples, we have specially summarized many other excellent g-C_3N_4 based nanomaterials in **Table 2**.

Volatile Organic Compounds (VOCs) Removal

Apart from the liquid-phase Fenton reaction, Li et al. (2016) constructed a solid-gas interfacial Fenton system, which is joint with an alkalized g-C_3N_4 based photocatalyst, converting the photogenerated H_2O_2 into reactive oxygen species (ROS). This powerful case contains light acting as driving force, alkalized g-C_3N_4-based photocatalyst as an *in-situ* H_2O_2 collector and surface-coated Fe^{3+} as a trigger for H_2O_2 conversion, thus achieving efficient activity of VOCs photodegradation. For instance, taking the photo-oxidation of isopropyl alcohol as a model. Specifically, **Figure 6A** showed the generation rate and apparent quantum yield (AQY) of acetone and CO_2 at about 420 nm of each CNK-OH&Fe catalyst with various Fe^{3+} loadings. Notably, the CNK-OH&Fe samples exhibited an increasing photocatalytic capacity accounting for the loading amount of Fe^{3+}. Consequently, when the loading amount 1.4 wt%, it exhibited the optimal efficiency, signifying the increasing amount of Fe^{3+} loading not only promoting the utilization rate of photoelectron as well as suppressing the light absorption of catalyst. The IPA photooxidation rate of the optimal CNK-OH&Fe sample achieved ca. 270 folds higher than that of pristine C_3N_4 (**Figure 6B**). In **Figure 6C**, the generating H_2O_2 was difficult to be observed over CNK-OH&Fe, attributing to the generated H_2O_2 quickly reacting with Fe^{2+} and the photoelectrons quickly reducing Fe^{3+} to form ·OH radicals. To confirm the truth of H_2O_2 converting into ·OH radicals over CNK-OH&Fe, EPR test were performed. It was found that apart from the direct ·OH formation of surface hydroxyl radicals inducing from holes, the CNK-OH&Fe indeed triggered the Fe^{2+} and H_2O_2 converting into ·OH. On one hand, the enhanced efficiency was arising from the conversion of electrons promoting the generation of reactive radicals (e.g., ·OH and $\cdot O_2^-$ radicals) via the solid-gas interfacial Fenton process. On the other hand, the hydroxyl and Fe^{3+} species determined the *in-situ* protons production and Fe^{2+}/Fe^{3+} formation. In **Figure 6D**, the amount of hydroxyl radicals over CNK-OH&Fe was ca. 4.0 times than that of CNK-OH. **Figure 6E** elaborately illustrated the possible mechanism over CNK-OH&Fe catalyzed isopropanol conversion. As to quantum yield, in **Figure 6F**, compared with the pristine C_3N_4, more than two orders of magnitude of conversion rate were obtained, which is equivalent to AQY of 49% around 420 nm. In addition, it is expected that this discovery is not only unique for C_3N_4-based nanomaterials, but provide a useful guidance for other semiconductors which can be alkalized on surface (e.g., WO_3 and $SrTiO_3$) should also provide the same light-driven Fenton process. It is expected that this will open a low economic cost and facile way to employ solar energy to effectively eliminate gaseous organic pollutants.

Photo-Fenton-Like Membranes for Wastewater Treatment

Membrane separation, a potential water treatment technology that has caused global attention to energy shortages and environmental pollution crises. In the last few decades, a vast amount of polymer and inorganic membranes have been deeply developed. Particularly, reverse osmosis (RO), plays a pivotal role in the generation of high-standard purified water, and simultaneously removes a vast number of contaminants (e.g., total dissolved solids, pathogens and organic pollutants).

In membrane development history, the thin film composite (TFC) polyamide membranes, thin film nanocomposite (TFN) membranes, molecular layer-by-layer (mLBL) membranes and self-assembled artificial water channels, carbon nanotubes (CNTs), microporous metal-organic frameworks (MOFs), graphene, graphene oxide, and MoS_2 incorporated membranes have been deeply developed and studied; however, to meet all the demands of high-quality membranes including high selectivity, evitable stability and anti-fouling capabilities as well as high permeation flux, is still a huge challenge (Yang et al., 2016, 2018; Tang et al., 2018).

Interestingly, carbonaceous materials are gradually recognized as promising candidates for designing high-performance membranes, including of 1D carbon nanotubes,

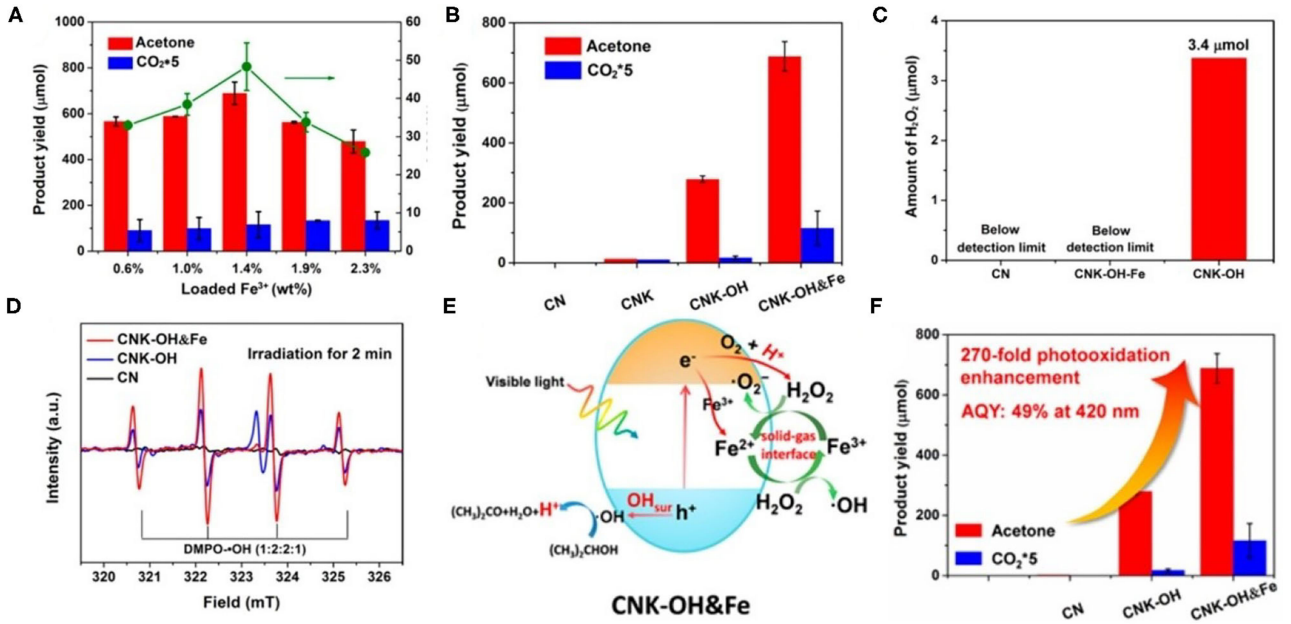

FIGURE 6 | (A) Product yield and AQY of CNK-OH&Fe as a function of Fe^{3+} loading. **(B)** Photooxidation efficiency of various C_3N_4-based photocatalysts. **(C)** Yield of H_2O_2 production over C_3N_4-based samples. **(D)** EPR spectra of DMPO-·OH of different samples. **(E)** Proposed mechanism of solid-gas interfacial Fenton reaction over CNK-OH&Fe. **(F)** Photooxidation performance of various C_3N_4-based photocatalysts. Copied with permission (Li et al., 2016). Copyright 2016, ACS.

2D graphene as well as its derivatives. However, for the practical application of carbon materials, it is limited by the difficulty of manufacturing densely arranged nanostructures. In addition, as to graphene-based membranes, it is necessary to greatly enhance the permeability and structural stability of the membrane. Therefore, it is of paramount importance to constructing membranes with feasible mass transfer resistance and water permeation flux. It is worth noting that graphite carbon nitride (g-C_3N_4) is expected to establish a new platform for the development of innovative membranes with excellent separation and self-cleaning properties, especially ultra-thin g-C_3N_4 nanosheets. On this condition, for the first time, Lan et al. (2019) innovatively manufactured g-C_3N_4-based catalytic membrane by soft self-assembly method for water purification. This membrane is mainly based on the nanochannels in g-C_3N_4 nanosheets and heterogeneous catalysis engaging in Fe-containing polyoxometalates. As shown in **Figure 7A**, the synthetic method of photo-Fenton-like membrane has been briefly described. Continuous modification of large amounts of g-C_3N_4 is beneficial to forming g-C_3N_4 sol (step II). Afterwards, customized g-C_3N_4 sol molecules with abundant amino and hydroxyl functional groups, provide enough active sites for Fe-POM nucleation (step III). After that, the self-assembly of the dispersion is filtered through a polycarbonate filter membrane to perform a carbonitride-based membrane treatment (Step IV). As shown in **Figures 7B–E**, the performance of POM incorporated into a g-C_3N_4 membrane was evaluated by pumping wastewater into membrane. First, the effect of carbon nitride microstructure was studied. As shown in **Figure 7B**, MB molecules can be completely removed from the water by g-C_3N_4 membrane. Compared with the melamine-derived membrane, the urea-derived sample showed much better removal efficiency. Moreover, the versatility of Ug-C_3N_4/Fe-POMs membranes in water purification was tested by filtering various dye molecules, as shown in **Figure 7C**. The results indicated that the synthesized membranes are capable of intercepting methyl blue (MB), Congo red (CR), methyl orange (MO), and rhodamine B (RhB) is extremely effective. In **Figure 7D**, the unique nanochannels in Ug-C_3N_4/Fe-POM ensured that contaminant molecules are completely removed through each filtration process. Therefore, if coupled with light irradiation and H_2O_2, this membrane exhibited stable water flux and good repelling ability (**Figure 7E**). In addition, a possible mechanism was proposed in **Figure 7F**. It was revealed that periodic atomic vacancies and structural defects in tri-s-triazine are conducive to the nanopores on the surface of the g-C_3N_4 layer. It is convinced that the gap between layers of carbon nitride provided a shortcut to dyes molecular diffusion. The modification of Fe-POMs significantly improved the separation performance of carbon nitride. In actual sewage treatment, the membranes were verified by pumping actual textile wastewater (initial COD: 290 mg L^{-1}) over U-g-C_3N_4/Fe-POMs membranes. Generally, the greater the amount of Fe-POM in the membrane, the higher the rejection rate, and the smaller the permeation flux of water (**Figure 7G**). As can be seen from **Figure 7H** that the addition of Fe-POMs posed a significant impact on the COD removal performance. Therefore, the U-gC_3N_4/Fe-POMs membrane maintained the same COD rejection rate and permeable flux after five

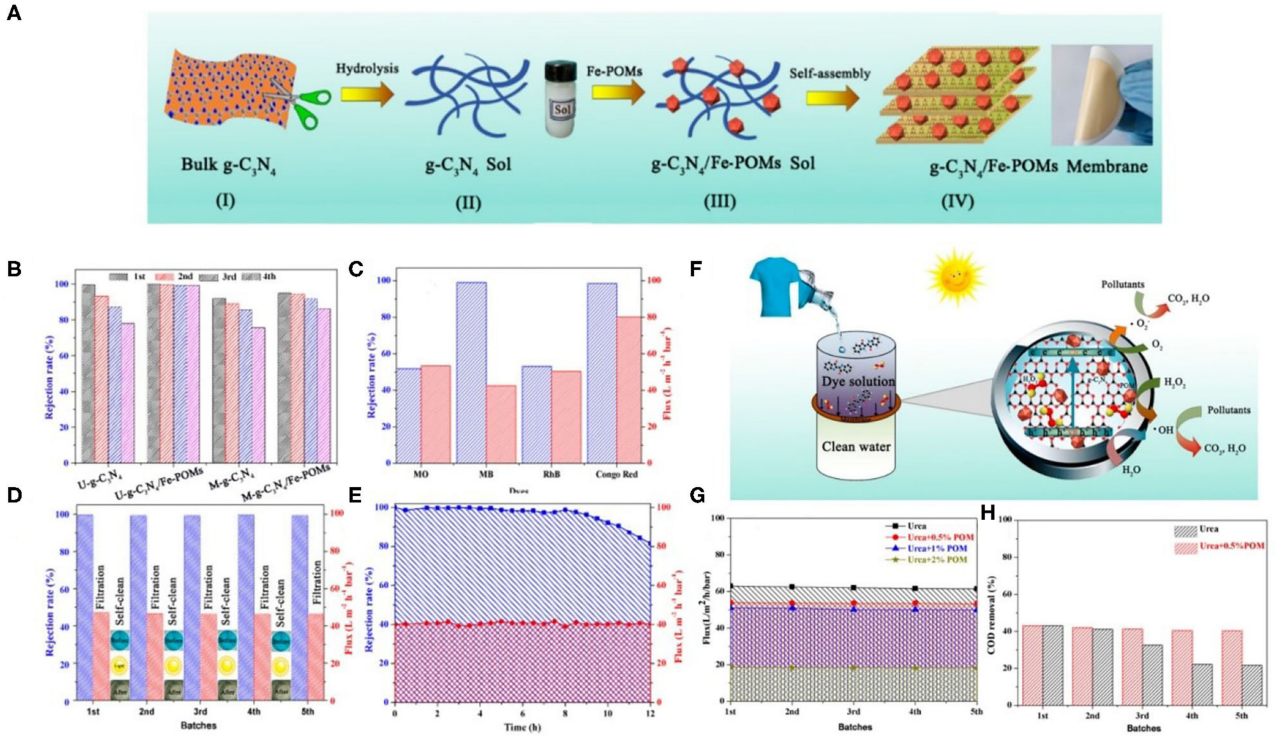

FIGURE 7 | (A) Schematic illustration of synthesis methodology of g-C_3N_4/Fe-POMs membranes. **(B)** Dye removal efficiency over different carbon-nitride-based membranes. **(C)** Filtration ability for U-g-C_3N_4/Fe-POMs membranes over various dye solutions. **(D)** Intermittent combination of membrane separation and photocatalytic oxidation process. **(E)** Treating MB solution by U-g-C_3N_4/Fe-POMs membranes with the aid of light and H_2O_2; **(F)** Possible mechanism of water purification over U-g-C_3N_4/Fe-POMs membranes. **(G)** Influence of Fe-POMs content on the water permeation flux. **(H)** COD removal rate of U-g-C_3N_4 and U-g-C_3N_4/1% Fe-POMs membranes in batch filtration experiments. Copied with permission (Lan et al., 2019). Copyright 2019, ACS.

batches of treatment. It well reveals the merits of self-assembled photo-Fenton membrane based on Fe-POM. Overall, this work provides a viable way to develop catalytic carbonitride-based membranes for water purification.

In this section, graphite carbon nitride (g-C_3N_4) nanomaterials were reviewed for the application of photo-Fenton process in removing organic pollutant, volatile organic compounds (VOCs) removal and membrane separation for wastewater. If irradiated by visible light or solar light, the photo-generated electrons facilitated the cycle of Fe^{3+}/Fe^{2+}, leading to the enhanced efficiency of organic pollutant and VOCs removal, which is attributed to the simultaneous photocatalytic effect as well as photo-Fenton oxidation process. According to this line of thought, g-C_3N_4 can be a promising candidate not only in organic pollutant removal but also assist in membrane separation and self-cleaning.

REDUCED GRAPHENE OXIDE (RGO)-BASED PHOTOCATALYTIC FENTON REACTION

Graphene has been recognized as an excellent candidate supporting material owing to its unique physical properties, such as a high electric potential density, electron mobility, and optical absorption (Nair et al., 2008; Mayorov et al., 2011). In the field of environmental remediation, for instance, graphene is usually employed as a good support for loading nanomaterials, such as TiO_2, ZnO, Fe_2O_3, CdS, Co_3O_4, and CdSe, etc. (Xiang et al., 2012; Guo et al., 2013) With the assistance of graphene, these nanocomposites can be uniformly dispersed onto graphene nanosheets and suppress aggregation, thus enhancing the catalytic efficiency because of excellent specific area and electrical conductivity (Wang et al., 2016). In the broad sense of Fenton process, two-dimensional graphene nanosheets and three-dimensional graphene hydrogel or aerogel have been deeply investigated. In the last decade, graphene-based nanocomposites, such as Fe_2O_3/graphene oxide and Fe_3O_4/RGO composites have been widely studied in removing organic pollutants (Xiang et al., 2012; Qiu et al., 2016b). These reported graphene-based photocatalysts show excellent photocatalytic activity, which is due to the transfer of photogenerated charge from the NPs surface to the graphene surface, thereby promoting the separation of electron-hole pairs and the generation of additional ·OH radicals. In addition, the combination of the aromatic ring of rGO and organic pollutants mainly comes into being π-π interaction and electrostatic interaction, which is conducive to the degradation process (Zhang et al., 2009; Sun

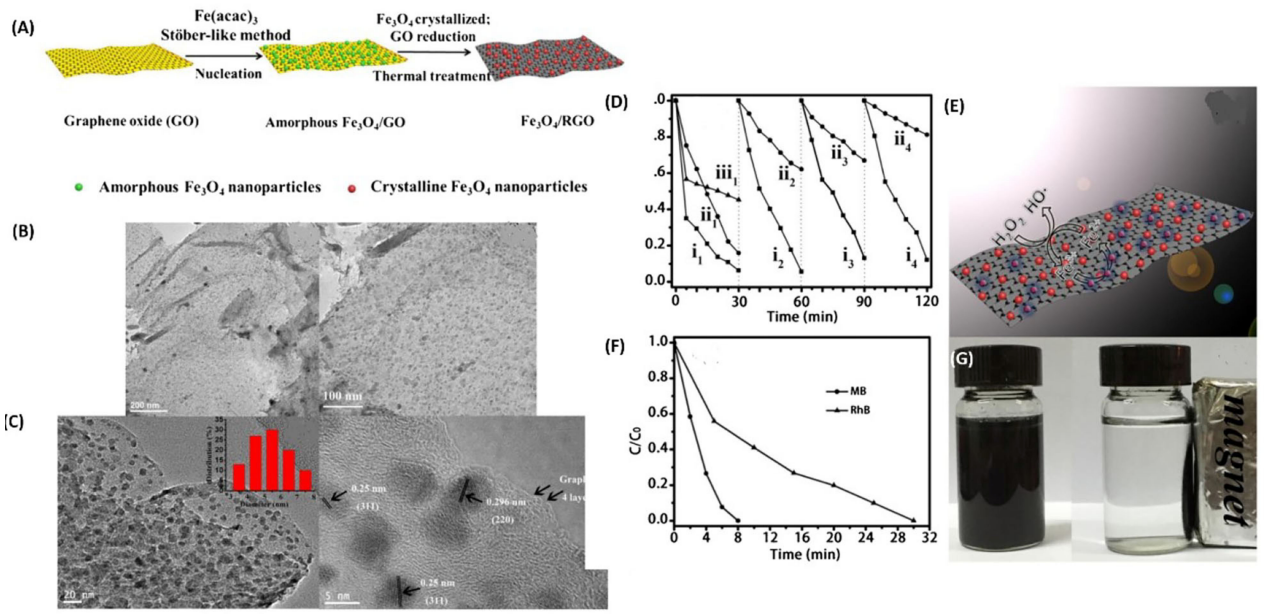

FIGURE 8 | (A) Synthetic route of Fe_3O_4/RGO nanomaterials; **(B)** TEM image and **(C)** HRTEM image of Fe_3O_4/RGO nanomaterials (Inset: particle size distribution of the loaded Fe_3O_4 nanoparticles); **(D)** Cycling test of Fe_3O_4/RGO and commercial Fe_3O_4 for degradation of MO irradiated by solar light; **(E)** Possible proposed photo-Fenton process mechanism of Fe_3O_4/RGO; **(F)** Photo-Fenton degradation of 10 mg/L MB and 10 mg/L RhB; **(G)** Magnetic recycle of Fe_3O_4/RGO photocatalyst. Copied with permission (Qiu et al., 2016b). Copyright 2016, Elsevier.

et al., 2020). Especially, Fe_2O_3, FeOOH, and Fe_3O_4 have been reported effective in Fenton reaction. Additionally, the three-dimensional graphene-based hydrogels, as well as aerogels have been investigated a lot in photo-Fenton like reaction. In this section, we will clarify them gradually.

Two-Dimensional Graphene-Based Nanomaterials

In 2016, Wang et al. (2016) prepared Fe_3O_4@HG with hydrophilic graphene (HG) and Fe_3O_4, which presented high removal efficiency of methyl orange (MO), owing to the rapid transference of photo-generated electrons on the surface of HG to promote the conversion efficiency of Fe^{3+}/Fe^{2+}. Further, Liu et al. (2017a) developed α-Fe_2O_3 loaded graphene oxide (GO) nanosheets through a facile hydrolysis process, which showed good Fenton-degradation efficiency for MB as well as rhodamine B, Orange II and Orange G, phenol, 2-nitrophenol and 17-estradiol (E2). An et al. (2013a) synthesized graphene-$BiFeO_3$ composite for the photo-Fenton degradation of tetrabromobisphenol A. Moreover, Qiu et al. (2016b) innovatively adopted a Stöber-like method to synthesize ultra-dispersed Fe_3O_4 nanoparticles onto graphene, which was applied in photo-Fenton reaction and lithium-battery. As presented in **Figure 8A**, the *in-situ* grown Fe_3O_4 particles were uniformly dispersed on graphene layers via a Stöber-like method. The morphology and structure of the Fe_3O_4/RGO composites have been characterized by TEM and HRTEM, as shown in **Figures 8B,C**, respectively. TEM images showed that the thickness of the RGO plate with highly dispersed Fe_3O_4 nanoparticles is ultrathin (**Figure 8B**). The HRTEM image of the Fe_3O_4/RGO composite (**Figure 8C**) showed that all nanoparticles are well-dispersed on graphene, and the size distribution shows an average size of 3–8 nm. HRTEM images show clear crystal lattices with a pitch of 0.250 and 0.296 nm, corresponding to the (311) and (220) planes, respectively. The photo-Fenton ability was conducted in the presence of H_2O_2 under the irradiation of solar light. Correspondingly, the result showed that the Fe_3O_4/RGO catalyst possessed superior photo-Fenton activity (98%) (**Figure 8D**). The possible mechanism has been illustrated in **Figure 8E**. Once irradiated by solar light, these electrons generating from dyes and Fe_3O_4 NPs transferred to the graphene; meanwhile, Fe^{3+} ions can easily be reduced by photo-electrons back to Fe^{2+}. Consequently, Fe^{2+} continue to react with H_2O_2 to produce more ·OH radicals on the surface of graphene (**Figure 8E**). As a result, the Fe_3O_4/RGO composites possessed an excellent photo-Fenton capacity for degradation of organic dyes (**Figure 8F**), which can be recycled by an extra magnetic (**Figure 8G**).

Three-Dimensional Graphene-Based Hydrogel or Aerogel

Besides the two-dimensional (2D) graphene-based heterogenous catalysts, to achieve the facile recycle of catalysts, three-dimensional (3D) graphene hydrogel or aerogel has been developed by many researchers, such as cobalt ferrite nanoparticles related graphene aerogel (Qiu et al., 2016a), graphene oxide (GO)-carbon nanotubes (CNTs)-FeOOH aerogel (Liu et al., 2017b), stretchable Fe_2O_3/graphene aerogels (Qiu

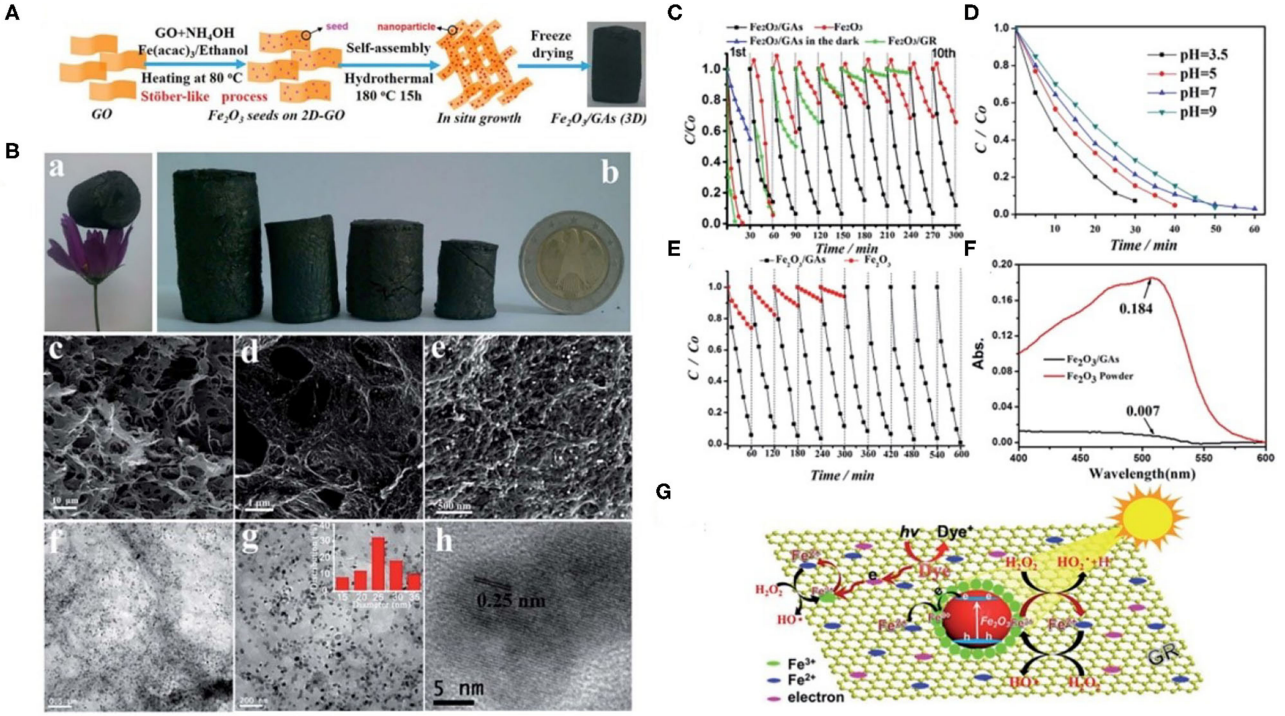

FIGURE 9 | (A) Illustration of synthesis methodology of Fe_2O_3/Gas; **(B)** (a) photographs of as-prepared Fe_2O_3/GAs; (b) images of Fe_2O_3/GAs prepared via different reaction volumes; (c) SEM and (d,e) FE-SEM image of Fe_2O_3/GAs (f,g) TEM, and (h) HR-TEM images of Fe_2O_3/GAs; **(C)** cycling test for the photo-Fenton degradation of MO; **(D)** photo-Fenton degradation of MO by Fe_2O_3/Gas; **(E)** cycle test for the photo-Fenton degradation of MO on different catalysts **(F)** Fe^{2+} detection of Fe_2O_3 powders and Fe_2O_3/GAs in the presence of 1,10-phenanthroline; **(G)** Photo-Fenton reaction model of Fe_2O_3/GAs. Copied with permission (Qiu et al., 2015). Copyright 2015, RSC.

et al., 2015), reduced graphene oxide nanosheet/FexOy/nitrogen-doped carbon layer aerogel (Yao et al., 2019), Fe_3O_4/RGO/PAM hydrogel (Dong et al., 2018c), etc.

Among these 3D graphene-based materials, especially, the graphene oxide aerogels have attracted tremendous attention in recent years, which is a new category of porous 3D framework, owing to its large surface-to-volume ratio, good electron mobility and conductivity, superior mechanical stability, and good adsorption capacity (Leary and Westwood, 2011). In a broad sense, 2D layered structures equipped with sp^2- and sp^3-hybridized carbon atoms are assembled in hexagonal rings, making graphene a useful building block for matrix self-assembly, whereas graphene aerogel can be effectively prevent graphene sheets from stacking. Generally, doping a metal oxide into porous 3D structure can effectively suppress stacking; meanwhile, these 3D aerogels possess huge surface area, fast mass and electron transfer kinetics, short diffusion paths in the matrix and good mechanical strength (Sui et al., 2012).

In addition, some previous studies have reported that nanoscale iron oxide in graphene aerogels, which possessed few defects, are especially effective for photo-Fenton degradation of phenols and more complex benzene ring compounds. For example, Qiu et al. (2015) reported three-dimensional (3D) Fe_2O_3 *in-situ* grown on graphene aerogels via Stöber-like method, as shown in **Figure 9A**. The obtained Fe_2O_3/GAs exhibited a 3D macroscopic appearance (**Figure 9B**, inset a) and an ultralight materials property. With the reaction volume increasing, the obtained Fe_2O_3/GAs increase in size (**Figure 9B**, inset b). The SEM image of Fe_2O_3/GAs indicated that the Fe_2O_3/GAs possessed a 3D macroporous structure (**Figure 9B**, inset c,d). Fe_2O_3 nanocrystals are well-embedded into graphene sheets (**Figure 9B**, inset e). TEM results further confirmed the highly dispersed Fe_2O_3 nanocrystals on the surface of graphene (**Figure 9B**, inset f,g). HRTEM image of Fe_2O_3/GAs revealed that d-spacing lattice fringes is ca. 0.25 nm, which corresponded to the (110) planes of Fe_2O_3 (**Figure 9B**, inset h). Subsequently, Fe_2O_3/GAs was investigated for the solar-light-driven Fenton reaction the in the presence of H_2O_2 for the degradation of 10 mg/L MO solution (**Figures 9C–E**). The highly photo-Fenton reaction activity was mainly caused by the conversion of Fe^{3+}/Fe^{2+} instead of the adsorption. Unlike Fe_2O_3/GR, the 3D-GAs can prevent the Fe^{2+} from dissolving in the solution owing to its channels and confinement effect. Besides the acidic conditions, the pH value can be adapted to neutral condition at 7.0, and the corresponding Fenton efficiency of Fe_2O_3/GAs still keeps at a high level, which is much higher than pristine Fe_2O_3 (**Figures 9D,E**). It is well-known that Fe^{3+}/Fe^{2+} cycle plays a crucial role in Fenton reaction. The excessive Fe^{3+} ions easily produce iron sludge in the aqueous solution, thus deactivating and poisoning the catalyst. In Fenton process, Fe^{3+} ions can

capture the photo-induced electrons and be reduced to Fe^{2+}, thus a high concentration of Fe^{2+} ions, which is complexed with phenanthroline can be detected in the solution (**Figure 9F**). The three-dimensional frame can effectively prevent the dissolution of iron. Once irradiated by solar light, the electrons can be both excited from dyes and Fe_2O_3 nanocrystals, which will transfer to the graphene (**Figure 9G**), leading to positive ions (e.g., Fe^{2+} and Fe^{3+}) adsorbed onto the negative-charge graphene. These Fe^{3+} ions will subsequently capture photo-induced electrons and react with H_2O_2 to produce Fe^{2+} ions again.

Additionally, Liu et al. (2018) used non-toxic sodium ascorbate as reductant to synthesize FeO(OH)/reduced graphene oxide aerogel (FeO(OH)-rGA) by means of facile and green-chemistry approach. The stable anchorage can ensure the circulation rate and reduce the leaching of iron, thereby ensuring the effective degradation of toxic phenolic compounds under visible light irradiation. Overall, the aerogel obtained not only has a stable structure, but also has significant catalytic activity for the degradation of phenolic organics at neutral pH. Besides this, Dong et al. (2018c) also developed a functional graphene hydrogel equipped with simultaneous photocatalytic Fenton reaction activity for the degradation of organic pollutants and adsorption for the heavy metal ions. These above-mentioned 3D graphene-based hydrogels or aerogels provide researchers a new pathway to process the wastewater treatment.

In a summary, reduced graphene oxide (RGO) based nanomaterials have been extensively employed in photocatalytic Fenton reaction, varying from two-dimensional (2D) nanosheets to three-dimensional (3D) hydrogels or aerogels. Especially, the 2D graphene nanosheets blocked the aggregation of iron oxide nanoparticles, benefiting the electron transferring on graphene and impeding the generation of iron sludge during photo-Fenton process. As to 3D graphene hydrogels and aerogels, it can effectively prevent the stacking of 2D graphene nanosheets by doping of metal ions. Moreover, its 3D-structured shape is suitable for multiple and simple recycling. It is expected that reduced graphene oxide will build a new platform for environmental remediation.

OTHER SEMICONDUCTORS-BASED PHOTOCATALYTIC FENTON REACTION

Except of the TiO_2-based, graphitic carbon nitride-based and graphene-based nanomaterials, some other semiconductor-based nanomaterials can work as effectively as well in photo-Fenton process, such as Ag (Chen et al., 2016; Zhu et al., 2018a,b), $BiVO_4$ (Xu et al., 2017; Li X. et al., 2018; Gao et al., 2019), ZnO (Choi et al., 2015; Ojha et al., 2017; Saleh and Taufik, 2019), $ZnFeO_4$ (Khadgi and Upreti, 2019; Palanivel et al., 2019), and $BiFeO_3$ (Luo et al., 2010; An et al., 2013b; Jia et al., 2018), etc. In this section, we will make a brief description, including of Ag-based nanomaterials, $BiVO_4$-based nanomaterials, $ZnFeO_4$ and $BiFeO_3$ based nanomaterials, which all perform well as photo-Fenton like catalysts.

Ag-Based Photo-Fenton Catalysts

In the past few decades, people have paid great attention to the research on the heterogeneous photo-Fenton process for the degradation of organic pollutants. As far as known, the high combination rate of photo-generated carriers will impede its photocatalytic efficiency. Thus, an idea is proposed that the joint of photo-Fenton catalysts with plasmonic materials, this issue might be solved.

Some researchers have reported that Ag/AgCl/Fe-S plasmonic catalyst could effectively degrade bisphenol A in photo-Fenton system under visible light irradiation (Liu et al., 2017c). Further, Zhu et al. (2018b) reported that a novel photo-Fenton catalyst of Ag/AgCl/ferrihydrite could degrade bisphenol A as well, which revealed that the loading of Ag/AgCl could accelerate the conversion of Fe^{3+}/Fe^{2+} by the photo-generated electrons transferring from Ag nanoparticles owning to the surface plasmon resonance (SPR) effect. Moreover, Chen et al. (2016) prepared Ag/hematite mesocrystal, which displayed a high photo-Fenton activity in the oxidation of RhB, MO and glyphosate under visible light irradiation.

$BiVO_4$-Based Photo-Fenton Catalysts

In recent years, $BiVO_4$ has been well-considered as a typical photocatalyst with narrow band gap. Due to its non-toxicity, good stability and photochemical properties, it has been extensively studied in the treatment of photocatalytic wastewater. In addition, $BiVO_4$ is a good candidate cocatalyst in photo-Fenton process; however, pure $BiVO_4$ is constrained by several drawbacks, such as a narrow visible light response range, low specific surface area, and rapid recombination of charged charges. Thus, various modification strategies have been adopted to investigate its potential application including doping ions, heterostructure fabrication, and precious metal deposition.

Specifically, Liu et al. (2017c) synthesized Fe(III) grafted $BiVO_4$ nanosheets, which was employed for the photodegradation of 2,4-dichlorophenol and antibiotics. The results showed that the Fe^{3+} species not only served as efficient electron scavengers, but also provided more active reaction sites. The detailed mechanism is briefly contained in **Figure 10A**. In **Figure 10B**, pure $BiVO_4$ merely could degrade ca. 60% of TC under visible-light irradiation. When the mass content of Fe(III) was 7%, the degradation efficiency can be up to 80%. Correspondingly, in **Figure 10C**, the TOC removal efficiency for 7% Fe(III)-BVO could be up to 48% after 60 min. Moreover, quinolones antibiotics, including CIP, GAT, and LVX were selected to be degraded. As shown in **Figures 10D–G**, the photocatalytic degradation efficiency of three antibiotics for Fe(III)-BVO is higher than that of pure BVO. Meanwhile, as an intermediate for the synthesis of pesticides and typical toxic organic compounds, photocatalytic degradation of 2,4-DCP possessed important practical significance for the treatment of wastewater.

$ZnFeO_4$ and $BiFeO_3$ Based Fenton Catalysts

$ZnFe_2O_4$ is a novel semiconductor, which possesses a band gap of about 1.9 eV, showing a visible light response, thus becoming

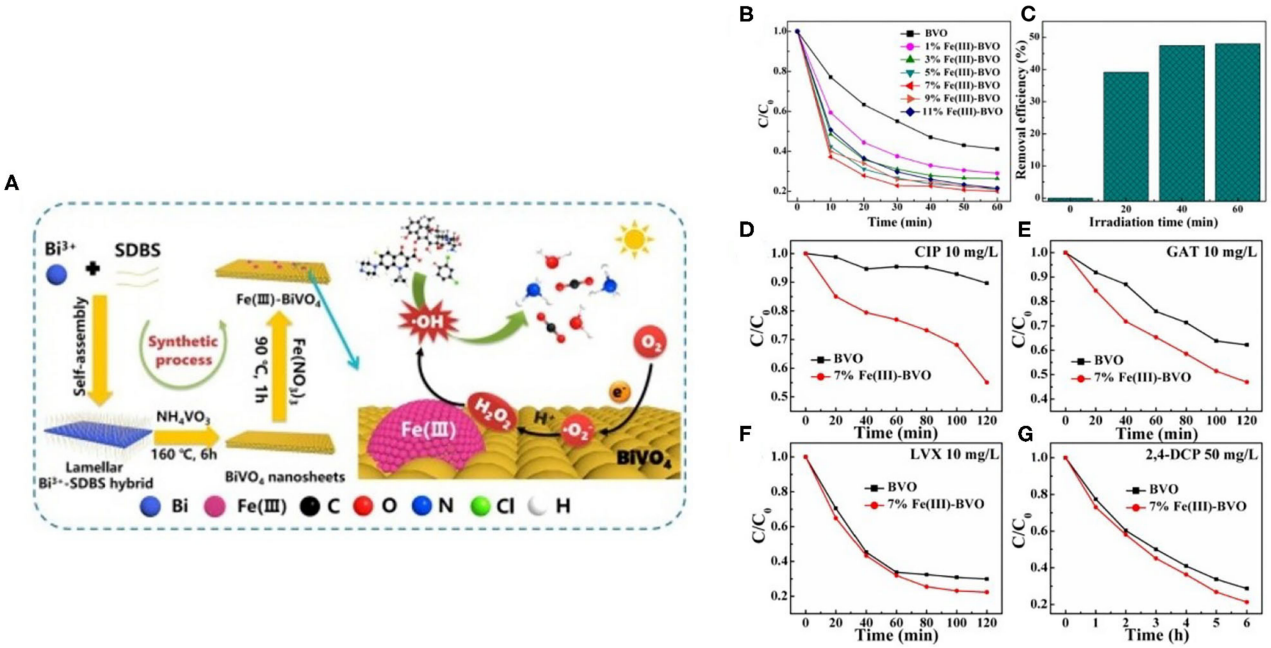

FIGURE 10 | (A) Systematic illustration of preparation method and mechanism; **(B)** photocatalytic degradation efficiency of TC using various contents of Fe(III)-BVO; **(C)** Total organic carbon (TOC) removal efficiency of TC by 7% Fe(III)-BVO photocatalyst and the photocatalytic activity of BVO and 7% Fe(III)-BVO for the degradation of **(D)** CIP, **(E)** GAT, **(F)** LVX, and **(G)** 2,4-DCP. Copied with permission (Liu et al., 2017c). Copyright 2019, Elsevier.

attractive in the field of visible light-driven photocatalysis (Sun et al., 2013; Zhu et al., 2016). Accordingly, both $ZnFe_2O_4$ and $ZnFe_2O_4$-based composites can act as photo Fenton-like catalysts to improve the degradation rate of organic pollutants in the presence of H_2O_2 (Su et al., 2012; Yao et al., 2014). For instance, Su et al. (2012) reported mesoporous $ZnFe_2O_4$ (meso-$ZnFe_2O_4$) prepared by a hydrothermal process. As to photocatalytic degradation of AOII, it showed that AOII almost completely removed in H_2O_2/visible light system after 2 h. It was revealed that high efficiency for AOII degradation was mainly attributed to the strong absorption of $ZnFe_2O_4$ in visible-light region and more generation amount of ·OH by H_2O_2. Further, Fu and Wang (2011) reported that they employed a feasible and facile one-step hydrothermal route to fabricate magnetic $ZnFe_2O_4$ graphene nanocomposites. The results showed that as prepared photocatalysts could serve as the photoelectrochemical catalysts for organic pollutants removal and the generator of hydroxyl radicals via the decomposition of H_2O_2 under visible light irradiation. Moreover, Chen H. et al. (2017) synthesized ZnO/$ZnFe_2O_4$ nanocomposite to degrade organic dye in the presence of H_2O_2 under near-infrared (NIR) irradiation. It was reported that ZnO/$ZnFe_2O_4$ nanocomposite performed well for the degradation of methyl orange under either UV, visible or NIR irradiation.

Besides $ZnFe_2O_4$-based nanocomposites, it is also discovered that $BiFeO_3$ perform as well in photo-Fenton like process. Generally, $BiFeO_3$ is recognized as one of the important semiconductors, which possess the ability for visible light response. Additionally, $BiFeO_3$ is widely accepted to be a promising visible-light-response photocatalyst for organic pollutant removal and hydrogen production (Bharathkumar et al., 2016). In Fenton-like process, Di et al. (2019) constructed Z-scheme heterojunction $Ag_2S/BiFeO_3$. The morphology of $Ag_2S/BiFeO_3$ was characterized by DF-STEM (**Figure 11A**). The corresponding elemental maps displayed as well. It showed a uniform elemental distribution of Bi, Fe, O and elements Ag and S. The result suggested that the Ag_2S nanoparticles have been successfully loaded onto the surface of $BiFeO_3$. Further, the photocatalytic and photo-Fenton efficiency was tested in **Figures 11B,C**, respectively. It was found that MO degradation was significantly enhanced with the addition of catalysts and H_2O_2. The specific mechanism of photocatalytic process and photo-Fenton process have been explained in **Figures 11D,E**. As far as known, the improved efficiency by photo-Fenton process mainly originated from the reduction of Fe^{3+} ions by photo-generated electrons, thus promoting the decomposition rate of H_2O_2. In addition, An et al. (2013a) prepared a nanoscale composite of $BiFeO_3$ and graphene, and used this composite to degrade tetrabromobisphenol A by photo-Fenton-like process, which showed that the graphene-$BiFeO_3$ composite exhibiting higher catalytic ability. Moreover, some researchers have found that $BiFeO_3$-based nanomaterials not only work on photo-Fenton process, but also perform well in sulfate radical based Advanced Oxidation Process (SR-AOP), revealing its vast potential in the field of wastewater treatment.

As above mentioned, some other novel Ag-based nanomaterials, $BiVO_4$-based nanomaterials, $ZnFeO_4$ and $BiFeO_3$ based nanocomposites were elucidated that effectively

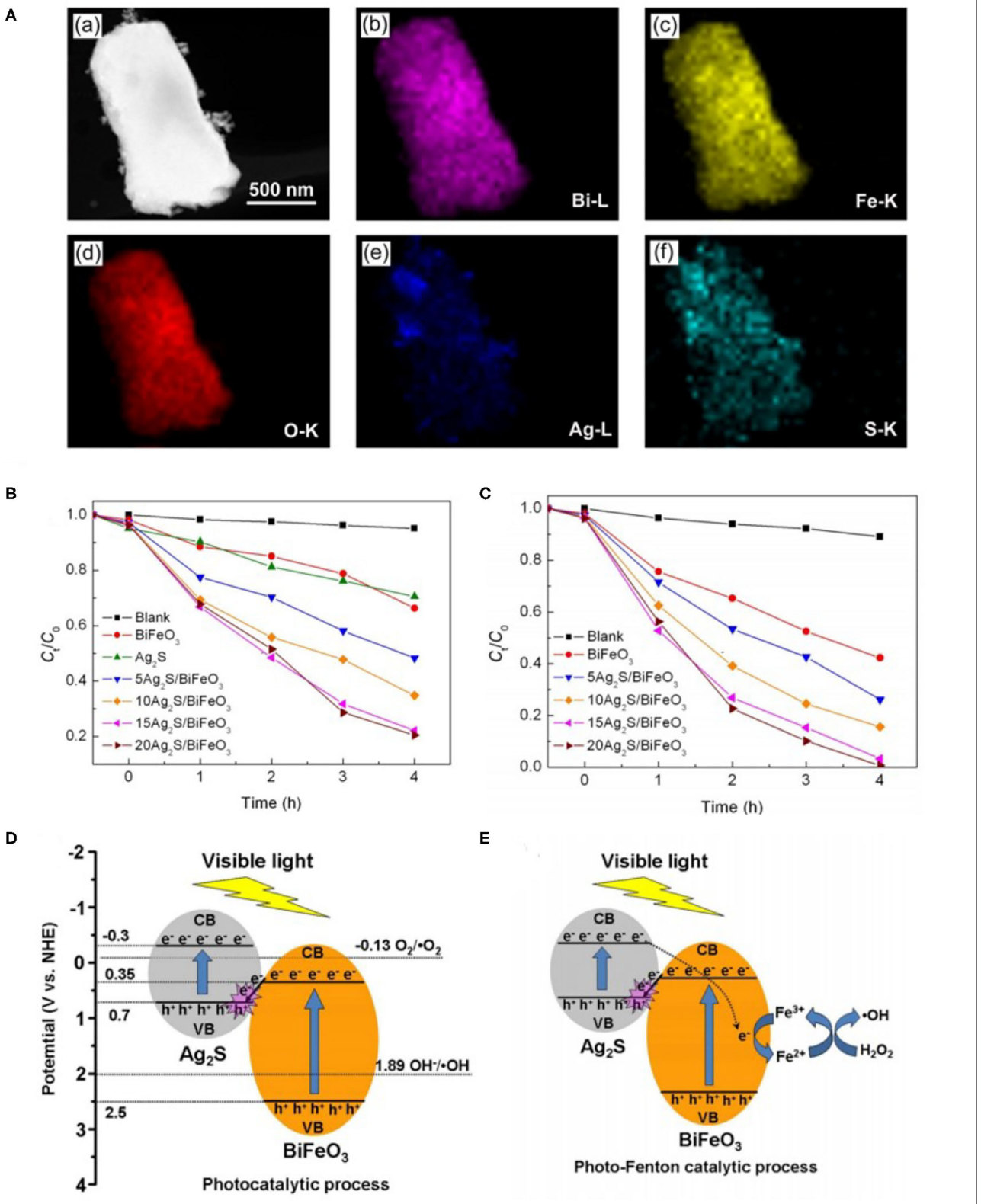

FIGURE 11 | (A) Dark-field scanning TEM image of 15% $Ag_2S/BiFeO_3$; (b–f) Corresponding elemental mapping images; **(B)** Photocatalytic activities of Ag_2S, $BiFeO_3$, and $Ag_2S/BiFeO_3$ composites for the degradation of MO under visible-light irradiation; **(C)** Photo-Fenton catalytic activities of $BiFeO_3$ and $Ag_2S/BiFeO_3$ composites for the degradation of MO in the presence of H_2O_2; Possible degradation mechanism of $Ag_2S/BiFeO_3$ composites **(D)** Photocatalytic process; **(E)** Photo-Fenton catalytic process. Copied with permission (Di et al., 2019). Copyright 2019, MDPI.

work on photo-Fenton reaction, stemming for their property acting as photocatalysts providing photo-electrons, which was involved in the transformation of Fe^{3+}/Fe^{2+}. On condition of this, there is no doubt that many other novel semiconductor photocatalyst can synergistically improve efficiency of the Fenton process if acting as the dual catalysts.

CONCLUSIONS AND OUTLOOK

In the last few decades, the photo-Fenton and photo-Fenton like process have been progressed a lot. The new developed photo-Fenton or photo-Fenton like process present higher efficiency than that of conventional ones. The key to solve the drawbacks of Fenton process is accelerating the transformation of Fe^{3+}/Fe^{2+}. Facing with this issue, the worldwide scientists have looked for many methodologies. Firstly, the TiO_2 and modified TiO_2 nanocomposites are able to perform as homogenous or heterogenous photo-Fenton cocatalysts, which focus on speeding up the cycle of Fe^{3+}/Fe^{2+}, leading to less iron sludge and higher removal efficiency for organic pollutant or bacteria. Secondly, to our best knowledge, graphitic carbon nitride is a new promising candidate in photocatalysis. Various types of iron oxide coupled g-C_3N_4 nanocomposites have been employed in wastewater treatment, VOCs removal and photo-Fenton like membrane separation. Thirdly, graphene is another excellent two-dimensional nanomaterial acting as good support for its good electron transferring capacity and large surface area. On premise that of good activity for 2D structure, three-dimensional graphene-based hydrogel or aerogel have been attempted in photo-Fenton and photo-Fenton like process. As to most of the 3D structural materials, the water-soluble Fe^{2+} ions can be easily anchored onto graphene, which explains why the photo-Fenton efficiency presents so good. In addition, some other semiconductors, such as Ag, $BiVO_4$, $ZnFeO_4$, and $BiFeO_3$ based nanomaterials have been reviewed briefly as well. In summary, the existing semiconductors, which are equipped with suitable band gap, large surface area, well-separated photo-generated carriers, which no doubt can be promising candidates in photo-Fenton process. Moreover, in recent years, some other alternative nanomaterials, such as metal disulfides, metal carbides, perovskites, etc. are all expected to provide good reference and efficacy in AOPs. However, facing the actual usage in industrial treatment, the sophisticated engineers usually focus more on the nanomaterials whether can be applied in actual sewage treatment on a large scale. Hence, the economic cost, recycling issues and stability need to be paid much attention to in the future development. In the field of actual wastewater treatment, the input energy and economic cost are both factors that we should consider in advance. Due to the injurious to human body and limited wavelength region of UV light, developing visible-light-response photocatalysts is a promising way to rationally treat wastewater, so as it can run at ambient temperature and pressure, utilizing atmospheric oxygen or H_2O_2 as oxidant. So far, synthesizing nanomaterials is of high cost, it is of great necessary to synthesize and adopt magnetic nanocomposites, such as Fe_3O_4-based and cobalt ferrite-based nanocomposites etc. Moreover, catalyst immobilization, which is closely associated with catalyst recovery and agglomeration, as well as the design of photocatalytic reactor are both key research points in the coming years. One possible strategy is heterogenous photo-Fenton like process with membrane processes (PMRs), and the other one is trying to prolong the contact time between solution and immobilized photocatalyst. Many efforts still need to be made to actual application of photo-Fenton-like process in the future development. If feasible, the nanomaterials in photo-Fenton-like process is expected to make a huge progress in environmental remediation.

AUTHOR CONTRIBUTIONS

CD and MX conceived the proposal of this manuscript. CD wrote the paper. MX and JZ gave suggestions on the writing. All authors contributed to the article and approved the submitted version.

FUNDING

This work was supported by the State Key Research Development Program of China (No. 2016YFA0204200), the National Natural Science Foundation of China (Nos. 21822603, 21677048, 21773062, 5171101651, and 21577036), the Shanghai Pujiang Program (No. 17PJD011), and the Fundamental Research Funds for the Central Universities (Nos. 22221818014 and 22A201514021).

REFERENCES

An, J., Zhu, L., Wang, N., Song, Z., Yang, Z., Du, D., et al. (2013a). Photo-Fenton like degradation of tetrabromobisphenol A with grapheneBiFeO$_3$ composite as a catalyst. *Chem. Eng. J.* 219, 225–237. doi: 10.1016/j.cej.2013.01.013

An, J., Zhu, L., Zhang, Y., and Tang, H. (2013b). Efficient visible light photo-fenton-like degradation of organic pollutants using *in situ* surface-modified $BiFeO_3$ as a catalyst. *J. Environ. Sci.* 25, 1213–1225. doi: 10.1016/S1001-0742(12)60172-7

Banić, N., Abramović, B., Krstić, J., Šojić, D., Lončarević, D., Guzsvány, V., et al. (2011). Photodegradation of thiacloprid using Fe/TiO_2 as a heterogeneous photo-Fenton catalyst. *Appl. Catal. B Environ.* 107, 363–371. doi: 10.1016/j.apcatb.2011.07.037

Bharathkumar, S., Sakar, M., and Balakumar, S. (2016). Experimental evidence for the carrier transportation enhanced visible light driven photocatalytic process in bismuth ferrite ($BiFeO_3$) one-dimensional fiber nanostructures. *J. Phys. Chem. C* 120, 18811–18821. doi: 10.1021/acs.jpcc.6b04344

Chen, C., Zhou, Y., Wang, N., Cheng, L., and Ding, H. (2015). $Cu_2(OH)PO_4$/g-C_3N_4 composite as an efficient visible light-activated photo-Fenton photocatalyst. *RSC Adv.* 5, 95523–95531. doi: 10.1039/C5RA15965B

Chen, H., Liu, W., and Qin, Z. (2017). ZnO/$ZnFe_2O_4$ nanocomposite as a broad-spectrum photo-Fenton-like photocatalyst with near-infrared activity. *Catal. Sci. Technol.* 7, 2236–2244. doi: 10.1039/C7CY00308K

Chen, Q., Chen, L., Qi, J., Tong, Y., Lv, Y., Xu, C., et al. (2019). Photocatalytic degradation of amoxicillin by carbon quantum dots modified $K_2Ti_6O_{13}$ nanotubes: effect of light wavelength. *Chin. Chem. Lett.* 30, 1214–1218. doi: 10.1016/j.cclet.2019.03.002

Chen, Q., Wu, P., Dang, Z., Zhu, N., Li, P., Wu, J., et al. (2010). Iron pillared vermiculite as a heterogeneous photo-Fenton catalyst for photocatalytic

degradation of azo dye reactive brilliant orange X-GN. *Sep. Purif. Technol*. 71, 315–323. doi: 10.1016/j.seppur.2009.12.017

Chen, X., Chen, F., Liu, F., Yan, X., Hu, W., Zhang, G., et al. (2016). Ag nanoparticles/hematite mesocrystals superstructure composite: a facile synthesis and enhanced heterogeneous photo-Fenton activity. *Catal. Sci. Technol*. 6, 4184–4191. doi: 10.1039/C6CY00080K

Chen, X., Lu, W., Xu, T., Li, N., Zhu, Z., Wang, G., et al. (2017). Visible-light-assisted generation of high-valent iron-oxo species anchored axially on g-C_3N_4 for efficient degradation of organic pollutants. *Chem. Eng. J*. 328, 853–861. doi: 10.1016/j.cej.2017.07.110

Choi, Y. I., Jung, H. J., Shin, W. G., and Sohn, Y. (2015). Band gap-engineered ZnO and Ag/ZnO by ball-milling method and their photocatalytic and Fenton-like photocatalytic activities. *Appl. Surf. Sci*. 356, 615–625. doi: 10.1016/j.apsusc.2015.08.118

Chow, C.-H., and Sze-Yin Leung, K. (2019). Transformations of organic micropollutants undergoing permanganate/bisulfite treatment: kinetics, pathways and toxicity. *Chemosphere* 237:124524. doi: 10.1016/j.chemosphere.2019.124524

Comer, B. M., and Medford, A. J. (2018). Analysis of photocatalytic nitrogen fixation on rutile TiO_2(110). *ACS Sustain. Chem. Eng*. 6, 4648–4660. doi: 10.1021/acssuschemeng.7b03652

Cui, Y., Ding, Z., Liu, P., Antonietti, M., Fu, X., and Wang, X. (2012). Metal-free activation of H_2O_2 by g-C_3N_4 under visible light irradiation for the degradation of organic pollutants. *Phys. Chem. Chem. Phys*. 14, 1455–1462. doi: 10.1039/C1CP22820J

Di, L., Yang, H., Xian, T., Liu, X., and Chen, X. J. N. (2019). Photocatalytic and photo-Fenton catalytic degradation activities of Z-scheme Ag_2S/$BiFeO_3$ heterojunction composites under visible-light irradiation. *Nanomater* 9:399. doi: 10.3390/nano9030399

Dong, C., Ji, J., Shen, B., Xing, M., and Zhang, J. (2018). Enhancement of H_2O_2 decomposition by the co-catalytic effect of WS2 on the Fenton reaction for the synchronous reduction of Cr(VI) and remediation of phenol. *Environ. Sci. Technol*. 52, 11297–11308. doi: 10.1021/acs.est.8b02403

Dong, C., Ji, J., Yang, Z., Xiao, Y., Xing, M., and Zhang, J. (2019). Research progress of photocatalysis based on highly dispersed titanium in mesoporous SiO_2. *Chin. Chem. Lett*. 30, 853–862. doi: 10.1016/j.cclet.2019.03.020

Dong, C., Lian, C., Hu, S., Deng, Z., Gong, J., Li, M., et al. (2018a). Size-dependent activity and selectivity of carbon dioxide photocatalytic reduction over platinum nanoparticles. *Nat. Commun*. 9:1252. doi: 10.1038/s41467-018-03666-2

Dong, C., Liu, J., Xing, M., and Zhang, J. (2018b). Development of titanium oxide-based mesoporous materials in photocatalysis. *Res. Chem. Intermediate* 44, 7079–7091. doi: 10.1007/s11164-018-3543-5

Dong, C., Lu, J., Qiu, B., Shen, B., Xing, M., and Zhang, J. (2018c). Developing stretchable and graphene-oxide-based hydrogel for the removal of organic pollutants and metal ions. *Appl. Catal. B Environ*. 222, 146–156. doi: 10.1016/j.apcatb.2017.10.011

Dong, H., Guo, X., and Yin, Y. (2018). A facile synthesis of goethite-modified g-C_3N_4 composite for photocatalytic degradation of tylosin in an aqueous solution. *Res. Chem. Intermediate* 44, 3151–3167. doi: 10.1007/s11164-018-3298-z

Duan, X., Su, C., Miao, J., Zhong, Y., Shao, Z., Wang, S., et al. (2018). Insights into perovskite-catalyzed peroxymonosulfate activation: maneuverable cobalt sites for promoted evolution of sulfate radicals. *Appl. Catal. B Environ*. 220, 626–634. doi: 10.1016/j.apcatb.2017.08.088

Esplugas, S., Bila, D. M., Krause, L. G. T., and Dezotti, M. (2007). Ozonation and advanced oxidation technologies to remove endocrine disrupting chemicals (EDCs) and pharmaceuticals and personal care products (PPCPs) in water effluents. *J. Hazard. Mater*. 149, 631–642. doi: 10.1016/j.jhazmat.2007.07.073

Fu, Y., and Wang, X. (2011). Magnetically separable $ZnFe_2O_4$-graphene catalyst and its high photocatalytic performance under visible light irradiation. *Ind. Eng. Chem. Res*. 50, 7210–7218. doi: 10.1021/ie200162a

Fujishima, A., and Honda, K. J. N. (1972). Electrochemical photolysis of water at a semiconductor electrode. *Nature* 238, 37–38. doi: 10.1038/238037a0

Gao, X., Ma, C., Liu, Y., Xing, L., and Yan, Y. (2019). Self-induced Fenton reaction constructed by Fe(III) grafted $BiVO_4$ nanosheets with improved photocatalytic performance and mechanism insight. *Appl. Surf. Sci*. 467–468, 673–683. doi: 10.1016/j.apsusc.2018.10.172

Giannakis, S., López, M. I. P., Spuhler, D., Pérez, J. A. S., Ibáñez, P. F., and Pulgarin, C. (2016). Solar disinfection is an augmentable, *in situ*-generated photo-Fenton reaction-part 2: a review of the applications for drinking water and wastewater disinfection. *Appl. Catal. B Environ*. 198, 431–446. doi: 10.1016/j.apcatb.2016.06.007

Guo, K., Zhang, J., Li, A., Xie, R., Liang, Z., Wang, A., et al. (2018). Ultraviolet irradiation of permanganate enhanced the oxidation of micropollutants by producing HO· and reactive manganese species. *Environ. Sci. Technol. Lett*. 5, 750–756. doi: 10.1021/acs.estlett.8b00402

Guo, S., Zhang, G., Guo, Y., and Yu, J. C. (2013). Graphene oxide-Fe_2O_3 hybrid material as highly efficient heterogeneous catalyst for degradation of organic contaminants. *Carbon* 60, 437–444. doi: 10.1016/j.carbon.2013.04.058

Guo, S., Zhu, Y., Yan, Y., Min, Y., Fan, J., and Xu, Q. (2016). Holey structured graphitic carbon nitride thin sheets with edge oxygen doping via photo-Fenton reaction with enhanced photocatalytic activity. *Appl. Catal. B Environ*. 185, 315–321. doi: 10.1016/j.apcatb.2015.11.030

Guo, T., Wang, K., Zhang, G., and Wu, X. (2019). A novel α- Fe_2O_3@g-C_3N_4 catalyst: synthesis derived from Fe-based MOF and its superior photo-Fenton performance. *Appl. Surf. Sci*. 469, 331–339. doi: 10.1016/j.apsusc.2018.10.183

He, D., Chen, Y., Situ, Y., Zhong, L., and Huang, H. (2017). Synthesis of ternary g-C_3N_4/Ag/γ-FeOOH photocatalyst: an integrated heterogeneous Fenton-like system for effectively degradation of azo dye methyl orange under visible light. *Appl. Surf. Sci*. 425, 862–872. doi: 10.1016/j.apsusc.2017.06.124

Hu, J., Zhang, P., An, W., Liu, L., Liang, Y., and Cui, W. (2019). In-situ Fe-doped g-C_3N_4 heterogeneous catalyst via photocatalysis-Fenton reaction with enriched photocatalytic performance for removal of complex wastewater. *Appl. Catal. B Environ*. 245, 130–142. doi: 10.1016/j.apcatb.2018.12.029

Hu, J.-Y., Tian, K., and Jiang, H. (2016). Improvement of phenol photodegradation efficiency by a combined g-C_3N_4/Fe(III)/persulfate system. *Chemosphere* 148, 34–40. doi: 10.1016/j.chemosphere.2016.01.002

Ikehata, K., and Li, Y. (2018). "Chapter 5-ozone-based processes," in *Advanced Oxidation Processes for Waste Water Treatment*, eds S. C. Ameta and R. Ameta (Fountain Valley, CA: Academic Press), 115–134.

Jain, B., Singh, A. K., Kim, H. Lichtfouse, E., Sharma, V. K. (2018). Treatment of organic pollutants by homogeneous and heterogeneous Fenton reaction processes. *Environ. Chem. Lett*. 16, 947–967. doi: 10.1007/s10311-018-0738-3

Jelic, A., Gros, M., Ginebreda, A., Cespedes-Sánchez, R., Ventura, F., Petrovic, M., et al. (2011). Occurrence, partition and removal of pharmaceuticals in sewage water and sludge during wastewater treatment. *Water Res*. 45, 1165–1176. doi: 10.1016/j.watres.2010.11.010

Jia, Y., Wu, C., Kim, D.-H., Lee, B. W., Rhee, S. J., Park, Y. C., et al. (2018). Nitrogen doped $BiFeO_3$ with enhanced magnetic properties and photo-Fenton catalytic activity for degradation of bisphenol a under visible light. *Chem. Eng. J*. 337, 709–721. doi: 10.1016/j.cej.2017.12.137

Khadgi, N., and Upreti, A. R. (2019). Photocatalytic degradation of microcystin-LR by visible light active and magnetic, $ZnFe_2O_4$-Ag/rGO nanocomposite and toxicity assessment of the intermediates. *Chemosphere* 221, 441–451. doi: 10.1016/j.chemosphere.2019.01.046

Khan, A. H., Kim, J., Sumarah, M., Macfie, S. M., and Ray, M. B. (2017). Toxicity reduction and improved biodegradability of benzalkonium chlorides by ozone/hydrogen peroxide advanced oxidation process. *Sep. Purif. Technol*. 185, 72–82. doi: 10.1016/j.seppur.2017.05.010

Kim, H.-E., Lee, J., Lee, H., and Lee, C. (2012). Synergistic effects of TiO_2 photocatalysis in combination with Fenton-like reactions on oxidation of organic compounds at circumneutral pH. *Appl. Catal. B Environ*. 115–116, 219–224. doi: 10.1016/j.apcatb.2011.12.027

Kim, J. R., and Kan, E. (2015). Heterogeneous photo-Fenton oxidation of methylene blue using CdS-carbon nanotube/TiO_2 under visible light. *J. Ind. Eng. Chem*. 21, 644–652. doi: 10.1016/j.jiec.2014.03.032

Klamerth, N., Malato, S., Agüera, A., and Fernández-Alba, A. (2013). Photo-Fenton and modified photo-Fenton at neutral pH for the treatment of emerging contaminants in wastewater treatment plant effluents: a comparison. *Water Res*. 47, 833–840. doi: 10.1016/j.watres.2012.11.008

Lan, H., Wang, F., Lan, M., An, X., Liu, H., and Qu, J. (2019). Hydrogen-bond-mediated self-assembly of carbon-nitride-based photo-Fenton-like membranes for wastewater treatment. *Environ. Sci. Technol.* 53, 6981–6988. doi: 10.1021/acs.est.9b00790

Leary, R., and Westwood, A. (2011). Carbonaceous nanomaterials for the enhancement of TiO_2 photocatalysis. *Carbon* 49, 741–772. doi: 10.1016/j.carbon.2010.10.010

Lee, Y., and von Gunten, U. (2010). Oxidative transformation of micropollutants during municipal wastewater treatment: comparison of kinetic aspects of selective (chlorine, chlorine dioxide, ferrateVI, and ozone) and non-selective oxidants (hydroxyl radical). *Water Res.* 44, 555–566. doi: 10.1016/j.watres.2009.11.045

Lei, X., You, M., Pan, F., Liu, M., Yang, P., Xia, D., et al. (2019). $CuFe_2O_4$@GO nanocomposite as an effective and recoverable catalyst of peroxymonosulfate activation for degradation of aqueous dye pollutants. *Chin. Chem. Lett.* 30, 2216–2220. doi: 10.1016/j.cclet.2019.05.039

Li, C., Wang, T., Zhao, Z.-J., Yang, W., Li, J.-F., Li, A., et al. (2018). Promoted fixation of molecular nitrogen with surface oxygen vacancies on plasmon-enhanced TiO_2 photoelectrodes. *Angew. Chem. Int. Ed.* 57, 5278–5282. doi: 10.1002/anie.201713229

Li, X., Liu, S., Cao, D., Mao, R., and Zhao, X. (2018). Synergetic activation of H_2O_2 by photo-generated electrons and cathodic Fenton reaction for enhanced self-driven photoelectrocatalytic degradation of organic pollutants. *Appl. Catal. B Environ.* 235, 1–8. doi: 10.1016/j.apcatb.2018.04.042

Li, Y., Ouyang, S., Xu, H., Wang, X., Bi, Y., Zhang, Y., et al. (2016). Constructing solid-gas-interfacial Fenton reaction over alkalinized-C_3N_4 photocatalyst to achieve apparent quantum yield of 49% at 420 nm. *J. Am. Chem. Soc.* 138, 13289–13297. doi: 10.1021/jacs.6b07272

Liu, R., Xu, Y., and Chen, B. (2018). Self-assembled nano-FeO(OH)/reduced graphene oxide aerogel as a reusable catalyst for photo-fenton degradation of phenolic organics. *Environ. Sci. Technol.* 52, 7043–7053. doi: 10.1021/acs.est.8b01043

Liu, Y., Jin, W., Zhao, Y., Zhang, G., and Zhang, W. (2017a). Enhanced catalytic degradation of methylene blue by α-Fe_2O_3/graphene oxide via heterogeneous photo-Fenton reactions. *Appl. Catal. B Environ.* 206, 642–652. doi: 10.1016/j.apcatb.2017.01.075

Liu, Y., Liu, X., Zhao, Y., and Dionysiou, D. D. (2017b). Aligned α-FeOOH nanorods anchored on a graphene oxide-carbon nanotubes aerogel can serve as an effective Fenton-like oxidation catalyst. *Appl. Catal. B Environ.* 213, 74–86. doi: 10.1016/j.apcatb.2017.05.019

Liu, Y., Mao, Y., Tang, X., Xu, Y., Li, C., and Li, F. (2017c). Synthesis of Ag/AgCl/Fe-S plasmonic catalyst for bisphenol A degradation in heterogeneous photo-Fenton system under visible light irradiation. *Chin. J. Catal.* 38, 1726–1735. doi: 10.1016/S1872-2067(17)62902-4

Luo, W., Zhu, L., Wang, N., Tang, H., Cao, M., She, Y. J. E., et al. (2010). Efficient removal of organic pollutants with magnetic nanoscaled $BiFeO_3$ as a reusable heterogeneous Fenton-like catalyst. *Environ. Sci. Technol.* 44, 1786–1791. doi: 10.1021/es903390g

Ma, J., Yang, Q., Wen, Y., and Liu, W. (2017). Fe-g-C_3N_4/graphitized mesoporous carbon composite as an effective Fenton-like catalyst in a wide pH range. *Appl. Catal. B Environ.* 201, 232–240. doi: 10.1016/j.apcatb.2016.08.048

Ma, M., Chen, L., Zhao, J., Liu, W., and Ji, H. (2019). Efficient activation of peroxymonosulfate by hollow cobalt hydroxide for degradation of ibuprofen and theoretical study. *Chin. Chem. Lett.* 30, 2191–2195. doi: 10.1016/j.cclet.2019.09.031

Matzek, L. W., and Carter, K. E. (2016). Activated persulfate for organic chemical degradation: a review. *Chemosphere* 151, 178–188. doi: 10.1016/j.chemosphere.2016.02.055

Mayorov, A. S., Gorbachev, R. V., Morozov, S. V., Britnell, L., Jalil, R., Ponomarenko, L. A., et al. (2011). Micrometer-scale ballistic transport in encapsulated graphene at room temperature. *Nano. Lett.* 11, 2396–2399. doi: 10.1021/nl200758b

Nair, R. R., Blake, P., Grigorenko, A. N., Novoselov, K. S., Booth, T. J., Stauber, T., et al. (2008). Fine structure constant defines visual transparency of graphene. *Science* 320:1308. doi: 10.1126/science.1156965

Ojha, D. P., Joshi, M. K., and Kim, H. J. (2017). Photo-Fenton degradation of organic pollutants using a zinc oxide decorated iron oxide/reduced graphene oxide nanocomposite. *Ceram. Int.* 43, 1290–1297. doi: 10.1016/j.ceramint.2016.10.079

Ortega-Liébana, M. C., Sánchez-López, E., Hidalgo-Carrillo, J., Marinas, A., Marinas, J. M., Urbano, F. J. (2012). A comparative study of photocatalytic degradation of 3-chloropyridine under UV and solar light by homogeneous (photo-Fenton) and heterogeneous (TiO_2) photocatalysis. *Appl. Catal. B Environ.* 127, 316–322. doi: 10.1016/j.apcatb.2012.08.036

Palanivel, B., Mudisoodum perumal, S. d., Maiyalagan, T., Jayarman, V., Ayyappan, C., and Alagiri, M. (2019). Rational design of $ZnFe_2O_4$/g-C_3N_4 nanocomposite for enhanced photo-Fenton reaction and supercapacitor performance. *Appl. Surf. Sci.* 498:143807. doi: 10.1016/j.apsusc.2019.143807

Qian, X., Ren, M., Fang, M., Kan, M., Yue, D., Bian, Z., et al. (2018a). Hydrophilic mesoporous carbon as iron(III)/(II) electron shuttle for visible light enhanced Fenton-like degradation of organic pollutants. *Appl. Catal. B Environ.* 231, 108–114. doi: 10.1016/j.apcatb.2018.03.016

Qian, X., Ren, M., Zhu, Y., Yue, D., Han, Y., Jia, J., et al. (2017). Visible light assisted heterogeneous Fenton-Like degradation of organic pollutant via α-FeOOH/mesoporous carbon composites. *Environ. Sci. Technol.* 51, 3993–4000. doi: 10.1021/acs.est.6b06429

Qian, X., Wu, Y., Kan, M., Fang, M., Yue, D., Zeng, J., et al. (2018b). FeOOH quantum dots coupled g-C_3N_4 for visible light driving photo-Fenton degradation of organic pollutants. *Appl. Catal. B Environ.* 237, 513–520. doi: 10.1016/j.apcatb.2018.05.074

Qiu, B., Deng, Y., Du, M., Xing, M., and Zhang, J. (2016a). Ultradispersed cobalt ferrite nanoparticles assembled in graphene aerogel for continuous photo-Fenton reaction and enhanced lithium storage performance. *Sci. Rep.* 6:29099. doi: 10.1038/srep29099

Qiu, B., Li, Q., Shen, B., Xing, M., and Zhang, J. (2016b). Stöber-like method to synthesize ultradispersed Fe_3O_4 nanoparticles on graphene with excellent photo-Fenton reaction and high-performance lithium storage. *Appl. Catal. B Environ.* 183, 216–223. doi: 10.1016/j.apcatb.2015.10.053

Qiu, B., Xing, M., and Zhang, J. (2015). Stöber-like method to synthesize ultralight, porous, stretchable Fe_2O_3/graphene aerogels for excellent performance in photo-Fenton reaction and electrochemical capacitors. *J. Mater. Chem. A* 3, 12820–12827. doi: 10.1039/C5TA02675J

Rincón, A.-G., and Pulgarin, C. (2004a). Bactericidal action of illuminated TiO_2 on pure Escherichia coli and natural bacterial consortia: post-irradiation events in the dark and assessment of the effective disinfection time. *Appl. Catal. B Environ.* 49, 99–112. doi: 10.1016/j.apcatb.2003.11.013

Rincón, A.-G., and Pulgarin, C. (2004b). Effect of pH, inorganic ions, organic matter and H_2O_2 on *E. coli* K12 photocatalytic inactivation by TiO_2: implications in solar water disinfection. *Appl. Catal. B Environ.* 51, 283–302. doi: 10.1016/j.apcatb.2004.03.007

Rincón, A.-G., and Pulgarin, C. (2006). Comparative evaluation of Fe^{3+} and TiO_2 photoassisted processes in solar photocatalytic disinfection of water. *Appl. Catal. B Environ.* 63, 222–231. doi: 10.1016/j.apcatb.2005.10.009

Safaei-Ghomi, J., Akbarzadeh, Z., and Teymuri, R. (2019). ZnS nanoparticles immobilized on graphitic carbon nitride as a recyclable and environmentally friendly catalyst for synthesis of 3-cinnamoyl coumarins. *Res. Chem. Intermediate* 45, 3425–3439. doi: 10.1007/s11164-019-03800-9

Sahar, S., Zeb, A., Liu, Y., Ullah, N., and Xu, A. (2017). Enhanced Fenton, photo-Fenton and peroxidase-like activity and stability over Fe_3O_4/g-C_3N_4 nanocomposites. *Chin. J. Catal.* 38, 2110–2119. doi: 10.1016/S1872-2067(17)62957-7

Saleh, R., and Taufik, A. (2019). Degradation of methylene blue and congo-red dyes using Fenton, photo-Fenton, sono-Fenton, and sonophoto-Fenton methods in the presence of iron(II,III) oxide/zinc oxide/graphene (Fe_3O_4/ZnO/graphene) composites. *Sep. Purif. Technol.* 210, 563–573. doi: 10.1016/j.seppur.2018.08.030

Shao, P., Duan, X., Xu, J., Tian, J., Shi, W., Gao, S., et al. (2017). Heterogeneous activation of peroxymonosulfate by amorphous boron for degradation of bisphenol S. *J. Hazard. Mater.* 322, 532–539. doi: 10.1016/j.jhazmat.2016.10.020

Shayegan, Z., Lee, C.-S., and Haghighat, F. (2018). TiO_2 photocatalyst for removal of volatile organic compounds in gas phase -a review. *Chem. Eng. J.* 334, 2408–2439. doi: 10.1016/j.cej.2017.09.153

Shen, B., Dong, C., Ji, J., Xing, M., and Zhang, J. (2019). Efficient Fe(III)/Fe(II) cycling triggered by MoO_2 in Fenton reaction for the degradation of dye molecules and the reduction of Cr(VI). *Chin. Chem. Lett.* 30, 2205–2210. doi: 10.1016/j.cclet.2019.09.052

Su, M., He, C., Sharma, V. K., Abou Asi, M., Xia, D., Li, X. Z., et al. (2012). Mesoporous zinc ferrite: synthesis, characterization, and photocatalytic activity with H_2O_2/visible light. *J. Hazard. Mater.* 211, 95–103. doi: 10.1016/j.jhazmat.2011.10.006

Sui, Z., Meng, Q., Zhang, X., Ma, R., and Cao, B. (2012). Green synthesis of carbon nanotube-graphene hybrid aerogels and their use as versatile agents for water purification. *J. Mater. Chem.* 22, 8767–8771. doi: 10.1039/c2jm00055e

Sun, T., Gong, M., Cai, Y., Zhang, L., Xu, Z., Zhang, D., et al. (2020). MCM-41-supported Fe(Mn)/Cu bimetallic heterogeneous catalysis for enhanced and recyclable photo-Fenton degradation of methylene blue. *Res. Chem. Intermediate* 46, 459–474. doi: 10.1007/s11164-019-03960-8

Sun, Y., Wang, W., Zhang, L., Sun, S., and Gao, E. (2013). Magnetic $ZnFe_2O_4$ octahedra: synthesis and visible light induced photocatalytic activities. *Mater. Lett.* 98, 124–127. doi: 10.1016/j.matlet.2013.02.014

Tan, C., Gao, N., Fu, D., Deng, J., and Deng, L. (2017). Efficient degradation of paracetamol with nanoscaled magnetic $CoFe_2O_4$ and $MnFe_2O_4$ as a heterogeneous catalyst of peroxymonosulfate. *Sep. Purif. Technol.* 175, 47–57. doi: 10.1016/j.seppur.2016.11.016

Tang, C. Y., Yang, Z., Guo, H., Wen, J. J., Nghiem, L. D., and Cornelissen, E. (2018). Potable water reuse through advanced membrane technology. *Environ. Sci. Technol.* 52, 10215–10223. doi: 10.1021/acs.est.8b00562

ThanhThuy, T. T., Feng, H., and Cai, Q. (2013). Photocatalytic degradation of pentachlorophenol on ZnSe/TiO_2 supported by photo-Fenton system. *Chem. Eng. J.* 223, 379–387. doi: 10.1016/j.cej.2013.03.025

Tryba, B., Morawski, A. W., Inagaki, M., and Toyoda, M. (2006). Mechanism of phenol decomposition on FeC TiO_2 and Fe TiO_2 photocatalysts via photo-Fenton process. *J. Photochem. Photobio. A Chem.* 179, 224–228. doi: 10.1016/j.jphotochem.2005.08.019

Vaiano, V., Sacco, O., Sannino, D., and Ciambelli, P. (2015). Nanostructured N-doped TiO_2 coated on glass spheres for the photocatalytic removal of organic dyes under UV or visible light irradiation. *Appl. Catal. B Environ.* 170-171, 153–161. doi: 10.1016/j.apcatb.2015.01.039

Wang, H., Xu, Y., Jing, L., Huang, S., Zhao, Y., He, M., et al. (2017). Novel magnetic $BaFe_{12}O_{19}$/g-C_3N_4 composites with enhanced thermocatalytic and photo-Fenton activity under visible-light. *J. Alloy. Compd.* 710, 510–518. doi: 10.1016/j.jallcom.2017.03.144

Wang, J., and Wang, S. (2018). Activation of persulfate (PS) and peroxymonosulfate (PMS) and application for the degradation of emerging contaminants. *Chem. Eng. J.* 334, 1502–1517. doi: 10.1016/j.cej.2017.11.059

Wang, L., Jiang, J., Pang, S.-Y., Gao, Y., Zhou, Y., Li, J., et al. (2019). Further insights into the combination of permanganate and peroxymonosulfate as an advanced oxidation process for destruction of aqueous organic contaminants. *Chemosphere* 228, 602–610. doi: 10.1016/j.chemosphere.2019.04.149

Wang, P., Wang, L., Sun, Q., Qiu, S., Liu, Y., Zhang, X., et al. (2016). Preparation and performance of Fe_3O_4@hydrophilic graphene composites with excellent Photo-Fenton activity for photocatalysis. *Mater. Lett.* 183, 61–64. doi: 10.1016/j.matlet.2016.07.080

Wang, P., Zhao, G., Wang, Y., and Lu, Y. (2017). $MnTiO_3$-driven low-temperature oxidative coupling of methane over TiO_2-doped Mn_2O_3-Na_2WO_4/SiO_2 catalyst. *Sci. Adv.* 3:e1603180. doi: 10.1126/sciadv.1603180

Wang, Q., Wang, P., Xu, P., Li, Y., Duan, J., Zhang, G., et al. (2020). Visible-light-driven photo-Fenton reactions using Zn1-1.5xFexS/g-C_3N_4 photocatalyst: degradation kinetics and mechanisms analysis. *Appl. Catal. B Environ.* 266:118653. doi: 10.1016/j.apcatb.2020.118653

Wang, Z., Fan, Y., Wu, R., Huo, Y., Wu, H., Wang, F., et al. (2018). Novel magnetic g-C_3N_4/α-Fe_2O_3/Fe_3O_4 composite for the very effective visible-light-Fenton degradation of orange II. *RSC Adv.* 8, 5180–5188. doi: 10.1039/C7RA13291C

Xi, Z., Li, C., Zhang, L., Xing, M., and Zhang, J. (2014). Synergistic effect of Cu_2O/TiO_2 heterostructure nanoparticle and its high H_2 evolution activity. *Int. J. Hydrogen Energ.* 39, 6345–6353. doi: 10.1016/j.ijhydene.2014.01.209

Xiang, Q., Yu, J., and Jaroniec, M. (2012). Graphene-based semiconductor photocatalysts. *Chem. Soc. Rev.* 41, 782–796. doi: 10.1039/C1CS15172J

Xing, M., Xu, W., Dong, C., Bai, Y., Zeng, J., Zhou, Y., et al. (2018a). Metal sulfides as excellent co-catalysts for H_2O_2 decomposition in advanced oxidation processes. *Chem* 4, 1359–1372. doi: 10.1016/j.chempr.2018.03.002

Xing, M., Zhang, J., Qiu, B., Tian, B., Anpo, M., and Che, M. (2015). A brown mesoporous TiO_2-x/MCF composite with an extremely high quantum yield of solar energy photocatalysis for H_2 evolution. *Small* 11, 1920–1929. doi: 10.1002/smll.201403056

Xing, M., Zhou, Y., Dong, C., Cai, L., Zeng, L., Shen, B., et al. (2018b). Modulation of the reduction potential of TiO_2-x by fluorination for efficient and selective CH4 generation from CO_2 photoreduction. *Nano. Lett.* 18, 3384–3390. doi: 10.1021/acs.nanolett.8b00197

Xu, T., Zhu, R., Zhu, G., Zhu, J., Liang, X., Zhu, Y., et al. (2017). Mechanisms for the enhanced photo-Fenton activity of ferrihydrite modified with $BiVO_4$ at neutral pH. *Appl. Catal. B Environ.* 212, 50–58. doi: 10.1016/j.apcatb.2017.04.064

Yang, Z., Ma, X.-H., and Tang, C. Y. (2018). Recent development of novel membranes for desalination. *Desalination* 434, 37–59. doi: 10.1016/j.desal.2017.11.046

Yang, Z., Wu, Y., Wang, J., Cao, B., and Tang, C. Y. (2016). *In situ* reduction of silver by polydopamine: a novel antimicrobial modification of a thin-film composite polyamide membrane. *Environ. Sci. Technol.* 50, 9543–9550. doi: 10.1021/acs.est.6b01867

Yao, T., Jia, W., Feng, Y., Zhang, J., Lian, Y., Wu, J., et al. (2019). Preparation of reduced graphene oxide nanosheet/Fe_xO_y/nitrogen-doped carbon layer aerogel as photo-Fenton catalyst with enhanced degradation activity and reusability. *J. Hazard. Mater.* 362, 62–71. doi: 10.1016/j.jhazmat.2018.08.084

Yao, Y., Qin, J., Cai, Y., Wei, F., Lu, F., and Wang, S. (2014). Facile synthesis of magnetic $ZnFe_2O_4$-reduced graphene oxide hybrid and its photo-Fenton-like behavior under visible iradiation. *Environ. Sci. Pollut. Res.* 21, 7296–7306. doi: 10.1007/s11356-014-2645-x

Ye, Y., Yang, H., Wang, X., and Feng, W. (2018). Photocatalytic, Fenton and photo-Fenton degradation of RhB over Z-scheme g-C_3N_4/$LaFeO_3$ heterojunction photocatalysts. *Mater. Sci. Semicon. Proc.* 82, 14–24. doi: 10.1016/j.mssp.2018.03.033

Yu, J., Low, J., Xiao, W., Zhou, P., and Jaroniec, M. (2014). Enhanced photocatalytic CO_2-reduction activity of anatase TiO_2 by coexposed {001} and {101} Facets. *J. Am. Chem. Soc.* 136, 8839–8842. doi: 10.1021/ja5044787

Yu, L., Shao, Y., and Li, D. (2017). Direct combination of hydrogen evolution from water and methane conversion in a photocatalytic system over Pt/TiO_2. *Appl. Catal. B Environ.* 204, 216–223. doi: 10.1016/j.apcatb.2016.11.039

Yu, S., Wang, Y., Sun, F., Wang, R., and Zhou, Y. (2018). Novel mpg-C_3N_4/TiO_2 nanocomposite photocatalytic membrane reactor for sulfamethoxazole photodegradation. *Chem. Eng. J.* 337, 183–192. doi: 10.1016/j.cej.2017.12.093

Zhang, D., Gersberg, R. M., Ng, W. J., and Tan, S. K. (2014). Removal of pharmaceuticals and personal care products in aquatic plant-based systems: a review. *Environ. Pollut.* 184, 620–639. doi: 10.1016/j.envpol.2013.09.009

Zhang, L., Tian, B., Chen, F., and Zhang, J. (2012). Nickel sulfide as co-catalyst on nanostructured TiO_2 for photocatalytic hydrogen evolution. *Int. J. Hydrogen Energ.* 37, 17060–17067. doi: 10.1016/j.ijhydene.2012.08.120

Zhang, Y.-Y., He, C., Deng, J.-H., Tu, Y.-T., Liu, J.-K., and Xiong, Y. (2009). Photo-Fenton-like catalytic activity of nano-lamellar $Fe_2V_4O_{13}$ in the degradation of organic pollutants. *Res. Chem. Intermediate* 35:727. doi: 10.1007/s11164-009-0090-0

Zhao, J., Ji, M., Di, J., Zhang, Y., He, M., Li, H., et al. (2020). Novel Z-scheme heterogeneous photo-Fenton-like g-C_3N_4/FeOCl for the pollutants degradation under visible light irradiation. *J. Photochem. Photobio. A Chem.* 391:112343. doi: 10.1016/j.jphotochem.2019.112343

Zhao, Y., Zhao, Y., Shi, R., Wang, B., Waterhouse, G. I. N., Wu, L.-Z., et al. (2019). Tuning oxygen vacancies in ultrathin TiO_2 nanosheets to boost photocatalytic nitrogen fixation up to 700 nm. *Adv. Mater.* 31:1806482. doi: 10.1002/adma.201806482

Zhou, L., Wang, L., Zhang, J., Lei, J., and Liu, Y. (2016). Well-dispersed Fe_2O_3 nanoparticles on g-C_3N_4 for efficient and stable Photo-Fenton photocatalysis under visible-light irradiation. *Eur. J. Inorg. Chem.* 34, 5387–5392. doi: 10.1002/ejic.201600959

Zhou, Y., Yi, Q., Xing, M., Shang, L., Zhang, T., and Zhang, J. (2016). Graphene modified mesoporous titania single crystals with controlled and selective photoredox surfaces. *Chem. Commun*. 52, 1689–1692. doi: 10.1039/C5CC07567J

Zhu, K., Wang, J., Wang, Y., Jin, C., and Ganeshraja, A. S. (2016). Visible-light-induced photocatalysis and peroxymonosulfate activation over $ZnFe_2O_4$ fine nanoparticles for degradation of orange II. *Catal. Sci. Technol*. 6, 2296–2304. doi: 10.1039/C5CY01735A

Zhu, Y., Zhu, R., Xi, Y., Xu, T., Yan, L., Zhu, J., et al. (2018a). Heterogeneous photo-Fenton degradation of bisphenol A over Ag/AgCl/ferrihydrite catalysts under visible light. *Chem. Eng. J*. 346, 567–577. doi: 10.1016/j.cej.2018.04.073

Zhu, Y., Zhu, R., Yan, L., Fu, H., Xi, Y., Zhou, H., et al. (2018b). Visible-light Ag/AgBr/ferrihydrite catalyst with enhanced heterogeneous photo-Fenton reactivity via electron transfer from Ag/AgBr to ferrihydrite. *Appl. Catal. B Environ*. 239, 280–289. doi: 10.1016/j.apcatb.2018.08.025

Conflict of Interest: The authors declare that the research was conducted in the absence of any commercial or financial relationships that could be construed as a potential conflict of interest.